12-2011

Direct contact pyrolysis of hydrocarbons: A source of hydrogen and interesting carbon formations

Peter G. Faught
University of Nevada, Las Vegas

DIRECT CONTACT PYROLYSIS OF HYDROCARBONS:
A SOURCE OF HYDROGEN AND INTERESTING
CARBON FORMATIONS

By

Peter G. Faught

Bachelor of Science
University of Nevada, Las Vegas
2009

A thesis submitted in partial fulfillment
of the requirements for the

Master of Science Degree in Mechanical Engineering
Department of Mechanical Engineering
Howard R. Hughes College of Engineering

The Graduate College
University of Nevada, Las Vegas
December 2011

We recommend the thesis prepared under our supervision by

Peter G. Faught

entitled

Direct Contact Pyrolysis of Hydrocarbons: A Source of Hydrogen and Interesting Carbon Formations

be accepted in partial fulfillment of the requirements for the degree of

Master of Science in Mechanical Engineering
Department of Mechanical Engineering

Brendan O'Toole, Committee Chair

Robert Boehm, Committee Member

David Stahl, Committee Member

Allen Johnson, Graduate College Representative

Ronald Smith, Ph. D., Vice President for Research and Graduate Studies
and Dean of the Graduate College

December 2011

ABSTRACT

**DIRECT CONTACT PYROLYSIS OF HYDROCARBONS: A SOURCE OF
HYDROGEN AND INTERESTING CARBON FORMATIONS**

By

Peter G Faught

Dr. Brendan O'Toole, Examination Committee Chair
Associate Professor of Mechanical Engineering
University of Nevada, Las Vegas

The work detailed in this document looks at a novel liquid metal supported catalytic system for the generation of hydrogen by decomposition of ethanol through direct contact pyrolysis. The hydrogen is produced at relatively low temperatures (500-600°C) and has carbon and water as co-products. It should be noted that CO is not observed as a product at these low temperatures. This is to be contrasted with the hydrogen produced at higher temperature from ethanol which does contain carbon monoxide. The presence of carbon monoxide in hydrogen complicates fuel cell operation and catalytic chemical processes. Thus, the lack of CO in this process is advantageous.

In theory the process is slightly exothermic, however in actual practice the process will require a small amount of heat to be added to the system for the reaction to occur. This heat could be usefully provided by a solar facility or waste heat generated as a byproduct of an industrial process. Further, if the source of the ethanol is either biological or otherwise uses a carbon dioxide stream (e.g. syngas based production), this process can be seen as net carbon sequestering.

The intent of this work was to investigate four major concepts, the first being the design and testing of the liquid metal reactor and feed stock delivery system. This system

must produce hydrogen by decomposition of ethanol at temperatures in excess of 700°C, a relatively straight forward thermodynamic process.

Additionally, the system design was intended to test the effects on this process when transitional metals such as iron, nickel, and cobalt are added to the system as a catalyst. Of further interest is the unique way in which the catalyst is delivered and regenerated during the operation of the system.

Finally, we examine the morphology of the carbon co-products produced during the lower temperature catalytic reaction. These carbon products manifested themselves in varied particulate forms depending on the liquid metal medium and catalyst used. One of the more interesting forms observed, was a carbon nanotube (CNT) structure.

We conclude this work by examining potential changes for the second generation reactor design as well as potential uses and capture techniques for the carbon co-products produced by the process.

ACKNOWLEDGEMENTS

I would first like to thank Dr. Allen Johnson without whom none of this would be possible. Allen not only convinced me to pursue this degree, but also provided the funding to pay for it. More important to this work is the fact Allen also provided access to a lab, the majority of the components used in the system, and small budget to pay for the consumables used. Additionally, the autonomy Allen has granted me has both allowed and forced me to develop a completely new set of skills. This project has opened my eyes to a completely different way to apply my degrees in the future. Allen started as my employer, became my mentor, and I now proudly call him my friend.

Additionally, I would like to thank Dr. Brendan O'Toole for helping to get me into this program, as well as agreeing to be both my advisor and committee chair. Dr. O'Toole also has provided me a great deal of autonomy during this process while still being available when assistance was needed. His time helping edit this work is also greatly appreciated.

My sincere thanks to Dr. Robert Boehm and Dr. David Stahl for agreeing to be on my committee, I respect both of your opinions very much.

My thanks also go out to Dr. Longzhou Ma for not only his analysis work on the TEM, but also for taking the time to teach me the basic theory and operation of the TEM.

I would like to express my gratitude to Dr. Jian Ma and Dr. John Farley for the equipment contributed to this work.

I would also like to thank Amo Sanchez and Jim Norton, UNLV physics shop, and Kevin Nelson, UNLV mechanical engineering shop, for the use of their facilities and expertise.

Finally, I would like to thank my mother for her help and understanding the last 10 years and to say; better late than never mom, thanks for not spending the college fund on a condo in Boca.

PREFACE

**DIRECT CONTACT PYROLYSIS OF HYDROCARBONS: A SOURCE OF
HYDROGEN AND INTERESTING CARBON FORMATIONS**

By

Peter G Faught

Dr. Brendan O'Toole, Examination Committee Chair
Associate Professor of Mechanical Engineering
University of Nevada, Las Vegas

In today's world there is ever increasing pressure to end the dependency on fossil fuels. Synthetic fuels become of interest as fossil fuels become more costly. A fuel is any material capable of storing energy that can later be extracted to perform mechanical work. As such, hydrogen has been touted in many circles as the fuel source of the future. Hydrogen is an attractive fuel, having a very high specific energy and non-toxic combustion products.

Though there is a strong push to utilize hydrogen as a fuel, currently it is most commonly used as a chemical feedstock. Hydrogen is used in large quantities as a raw material in the chemical synthesis of ammonia, methanol, hydrogen peroxide, polymers, and solvents. Hydrogen can be produced from a variety of resources (water, fossil fuels, or biomass) and is a byproduct of other chemical processes. In the U.S. most hydrogen is produced by steam reformation of hydrocarbons, usually natural gas (methane). Other methods include generation by partial oxidation of coal or hydrocarbons, electrolysis of water, and recovery of byproduct hydrogen from other chemical processes.

Many of the end users of hydrogen purchase it as a liquid, which is vaporized as needed, instead of onsite production which requires a large scale investment in equipment. However, hydrogen is a tough material to transport and store. Thus,

strategies which convert easily transportable and storable intermediates, such as ethanol, have advantages. Recently, small on site hydrogen production systems have become increasingly attractive for chemical processes with small hydrogen requirements. One source, Universal Industrial Gases, Inc. notes:

The latest generation of highly packaged hydrocarbon reforming units, in particular those which employ an auto thermal generation process, which operates at relatively low-temperature and pressure, have made on-site hydrocarbon reforming a viable route to hydrogen production at much lower production rates than were considered commercially feasible just a few years ago [1].

These compact generators might be used as the sole source of hydrogen or as a supplement to other sources.

Several low temperature catalyzed reactions have been studied in recent years using alcohols as the hydrocarbon feed stock. Casanovas et al. (2008) investigated Auto-thermal generation of hydrogen from ethanol in a micro-reactor. Their system used a Co/ZnO catalyst in a low temperature regime (300-400 °C) [2]. Further, Kuen-Song Lin et al. (2011) conducted a study using a similar reactor design, however the catalyst used was CuO/ZnO, methanol was the hydrocarbon choice, and the system employed a even lower temperature regime (200-300 °C) [3].

In addition, environmental concerns have made the reduction of greenhouse gases, especially carbon monoxide, mandatory. The buzz word being used is **carbon sequestration**. Any new processes developed to produce synthetic fuels will have to have low emissions; additionally a system that operates carbon neutral or is net carbon sequestering would be highly desirable.

TABLE OF CONTENTS

LIST OF TABLES

LIST OF FIGURES

CHAPTER 1 INTRODUCTION

The work detailed in this document is actually the result of some fortunate timing. For a research professor like Dr. Johnson part of the job is looking for new projects and ways to fund them; as a result he had several concepts in mind that needed testing. These concepts come from a combination of his expertise in chemistry, his interest in materials science, and observations/discussions resulting from earlier work in liquid metals.

My contribution to this work comes from the fact that I am what university terms a non-traditional student. As such I bring a skill set in fabrication not normally possessed by a student. By combining our talents we were able to do this research without a primary funding source.

The reasoning behind this work is simple, by utilizing repurposed and borrowed equipment, available fabrication facilities, and a limited budget; an experimental system was designed and built to test several concepts in succession. Proof of concept would then be used to pursue funding opportunities. Although this paper is presented in sections all of the work was intended to be interdependent. The goal was to design a system that would cause a catalyzed reaction producing hydrogen and a controllable carbon byproduct, specifically carbon nanotubes.

1.1 Background

In this work we examine the thermal decomposition of ethanol as a method to generate hydrogen for subsequent utilization as a fuel or chemical feed stock. This system achieves thermal decomposition through direct contact pyrolysis of ethanol in a reactor design that utilizes a novel liquid metal supported catalytic system. This system will hereafter be referred to as a liquid metal reactor (LMR). The LMR allowed the

testing of the non-catalyzed pyrolysis reaction which was used as a baseline against which the catalyzed reactions would be compared.

Additionally, the delivery of the catalyst was tested using a phenomenon noticed in earlier liquid metals work. The design of this system allows for 1-2 second contact time between the feed gas and the liquid metal supported catalyst at which time the reaction occurs. Various catalysts were tested as a way of creating a lower temperature reaction to produce hydrogen that will also allow for the capture of carbon by-products in particulate form. It is believed that this design will allow for in-situ regeneration of the catalyst particles, thus eliminating long term catalyst stability problems (coking, carburization, etc.). Further, we believe the suspension of the catalytic particles may produce conditions favorable for the formation of carbon nanotubes (CNTs) or other useful carbon forms.

Finally, as mentioned earlier the output of the catalyzed reaction is intended to be hydrogen and controllable carbon forms. As such the process output is examined for 1) hydrogen production as a function of ethanol decomposition. 2) Morphology of the particulate carbon forms produced. 3) Temperature operating range before the onset of CO production.

1.2 Hydrogen Production

Currently, steam reforming of hydrocarbons (methane from natural gas being most prevalent) is the most commonly used method for hydrogen production. At high temperatures (700–1100 °C), steam (H_2O) reacts with methane (CH_4) to yield syngas, as shown in equation 1.1:

$$CH_4 + H_2O \rightarrow CO + 3\ H_2 + 206.1\ kJ/mol \qquad [1.1]$$

In a second stage, further hydrogen is generated through the lower-temperature water gas shift reaction (equation 1.2), performed at about 130 °C.

$$CO + H_2O \rightarrow CO_2 + H_2 - 41.2 \text{ kJ/mol} \qquad [1.2]$$
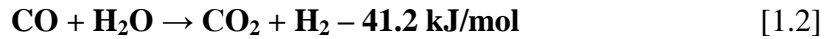
Essentially, the oxygen (O) atom is stripped from the additional water (steam) to oxidize CO to CO_2. This oxidation also provides energy to maintain the reaction. Additional heat required to drive the process is generally supplied by burning some portion of the methane [4]. Steam reforming generates carbon dioxide (CO_2) which is generally released into the atmosphere, a problematic practice in a world increasingly concerned about the release of greenhouse gases.

The production of hydrogen by steam reforming of pure ethanol (C_2H_5OH) has been widely investigated. Jordi et al. (2002) performed their investigation using a Co/ZnO catalyst [5], whereas Leclerc et al. (1998) reported that water to ethanol ratios in the range of 20:1 to 30:1 enhanced hydrogen selectivity and inhibited the production of undesirable products such as methane (CH_4), carbon monoxide (CO), acetaldehyde, ethylene and carbon [6]. Galvita et al. (2001) used water to ethanol molar ratios of 3:1 and 8.1:1, combined with Ni/MgO as a catalyst [7].

Here again the steam reforming process consists of two steps. Step one is the endothermic cracking process where ethanol and water react to form CO and H_2 as shown in equation 1.3:

$$C_2H_5OH + H_2O \rightarrow 2CO + 4H_2 + 298.5 \text{ kJ/mol} \qquad [1.3]$$
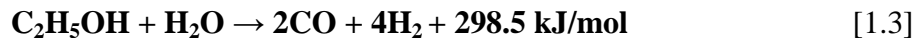
The water gas shift reaction (equation 1.2) is again used to increase overall hydrogen output as well as removing the CO from the product gas.

Direct pyrolysis of ethanol (no water added to the system) has also been studied for both hydrogen production and carbon forms such as soot. Pyrolysis in this case is simply thermal decomposition of ethanol in the absence of oxygen for the production of hydrogen.

Work performed by Esarte et al. has shown carbon monoxide to be a by-product of the pyrolysis of ethanol beginning at temperatures in excess of 600 °C. The CO production continues to rise as the temperature increases; hydrogen generation also increases with rising reaction temperatures [8]. In this case the basic reaction is taken as shown in equation 1.4:

$$\textbf{C}_2\textbf{H}_5\textbf{OH} \rightarrow \textbf{CH}_4 + \textbf{CO} + \textbf{H}_2 \textbf{ +92.4 kJ/mol} \qquad [1.4]$$
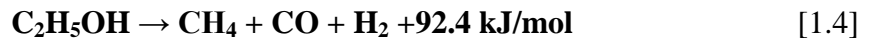
It should be noted however that small amounts of carbon dioxide (CO_2), ethene (C_2H_4), ethane (C_2H_6), and acetylene (C_2H_2) are noted in the product gas stream. These by-products are a result of simultaneous reactions with varying activation energies, and have been noted across a wide range of temperatures and conditions in most of the literature. While these by-products are a relatively small percentage of the output, the can be easily controlled by the addition of catalysts and temperature regulation.

Initial testing of our reactor design has shown the catalyzed reactions generate hydrogen at lower temperatures (500-600°C) and have carbon (C) and water (H_2O) as co-products as shown in equation 1.5:

$$\textbf{C}_2\textbf{H}_5\textbf{OH} \rightarrow \textbf{2C} + \textbf{2H}_2 + \textbf{H}_2\textbf{O} - \textbf{8.1 kJ/mol} \qquad [1.5]$$
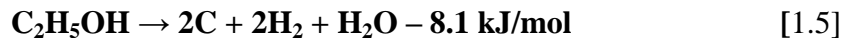
It should also be noted that CO is not observed as a product at these low temperatures, not showing up until around 700 °C.

When we examine equations 1.1 and 1.3 we see that the steam reforming process is endothermic, requiring energy to be added to the system for the reaction to occur. In contrast it can be seen from equation 1.5 our lower temperature reaction is slightly exothermic. The standard enthalpy of formation is used in thermo-chemistry to find the standard enthalpy change of reaction.

$$\Delta H° = \Sigma(v \times \Delta H_f°) \text{ (products) - } \Sigma(v \times \Delta H_f°) \text{ (reactants)} \qquad [1.6]$$

For example, for the reaction $CH_4 + 2 O_2 \rightarrow CO_2 + 2 H_2O$:

$$\Delta H_r° = [(1 \times \Delta H_f°_{(CO2)}) + (2 \times \Delta H_f°_{(H2O)})] \text{ (products) -}$$

$$[(1 \times \Delta H_f°_{(CH4)}) + (2 \times \Delta H_f°_{(O2)})] \text{ (reactants)} \qquad [1.7]$$

If the standard enthalpy of the products is less than the standard enthalpy of the reactants, the standard enthalpy of reaction will be negative. This implies that the reaction is exothermic. Similarly for an endothermic reaction, the standard enthalpy of reaction will be positive. Table 1 shows the heat of formation for the compounds of interest. Table 2 shows the reaction type (eq. 1.1-1.5).

Table 1 Heats of formation of select compounds

Substance	$\Delta H_f°$ (kJ/mol)	Substance	$\Delta H_f°$ (kJ/mol)
$CH_{4\,(g)}$	-74.8	$C_2H_5OH_{(l)}$	-277.7
$CO_{(g)}$	-110.5	$CO_{2\,(g)}$	-393.5
$H_2O_{(g)}$	-241.8	$C_{(s)}$	0
$H_2O_{(l)}$	-285.8	$H_{2\,(g)}$	0

Table 2 Reaction types

$CH_4 + H_2O \rightarrow CO + 3\ H_2 + 206.1 kJ/mol$ [1.1]	Endothermic
$CO + H_2O \rightarrow CO_2 + H_2 - 41.2\ kJ/mol$ [1.2]	Exothermic
$C_2H_5OH + H_2O \rightarrow 2CO + 4H_2 + 298.5\ kJ/mol$ [1.3]	Endothermic
$C_2H_5OH \rightarrow CH_4 + CO + H_2 + 92.4\ kJ/mol$ [1.4]	Endothermic
$C_2H_5OH \rightarrow 2C + 2H_2 + H_2O - 8.1\ kJ/mol$ [1.5]	Exothermic

In theory, once started our system should be self-sustaining. However, due to real world losses the system will require a small amount of additional heat. As mentioned in the abstract we believe this heat could be usefully provided by a solar facility or waste heat generated as a byproduct of an industrial process.

1.3 Catalysts

Catalysts make reactions happen; they augment the rate of chemical reactions without being consumed in the reaction. Using catalysts can change the speed of a reaction or allow for a more selective reaction. Proper selection of catalysts can speed up some reactions and not others, allowing the process to work more efficiently and often with less waste. Catalysis is regularly used to treat hazardous materials, thus minimizing the impact of industrial processes on the environment.

The purpose of a catalyst is to provide an alternative path for the reaction to occur. An increase in reaction rate is due to the fact that the activation energy for the alternative path is lower than the path followed in a non-catalyzed reaction. Figure 1.1 shows a graphical representation of the different reaction paths.
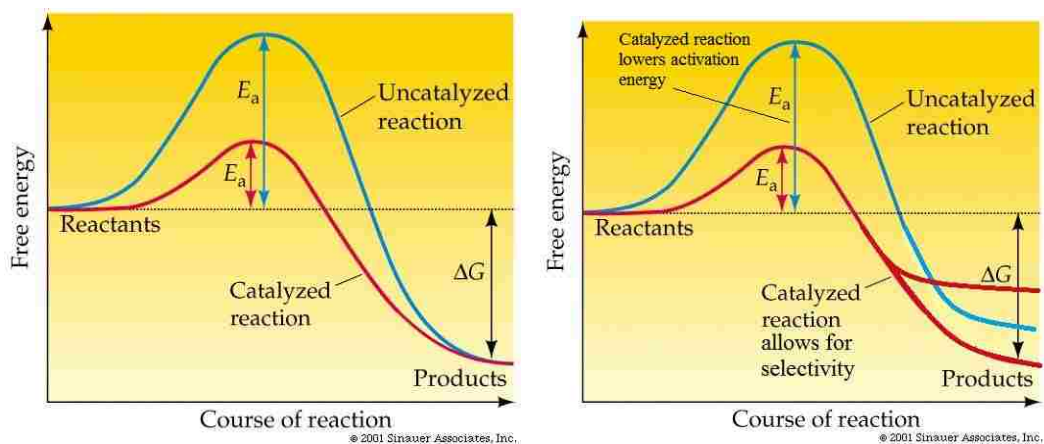
Figure 1.1 Course of reactions same and different end products [9].

Our system employs what is known as heterogeneous catalysis. This implies that the phase of the catalyst is different than the phase of the reactants. Most practical heterogeneous catalysts are solids, while most reactants take a gaseous or liquid form. Many heterogeneous catalysts are supported in or on a second material to increase the effectiveness or simply to increase the total surface area. Total surface area is important to reaction rates. Smaller particle size increases the effective surface area per a given mass of particles. Though the catalyst particles are not consumed by the reaction, they tend to become less effective over time or can be destroyed due to secondary processes such as coking. Coking is a process that covers the catalyst in polymeric by-products.

Transition metals/compounds are well known for their homogeneous and heterogeneous catalytic activity. Their ability to change oxidation state or, in the case of the metals, to adsorb and activate other substances on to their surface make them indispensable in industrial processes. We choose to test three transition metals as catalysts. Iron was picked for its high carbon content, while nickel and cobalt were obvious choices being regularly used both in the laboratory and industrial applications such as steam reformation.

In this reactor design the catalytic particles are suspended in the liquid metal support. The idea for this catalyst delivery method came from a discussion between Dr. Johnson and Dr. Eric Loewen about a phenomenon noticed during an unpublished LBE study [10]. At the end of a corrosion study of steel in LBE, Dr. Loewen decided to examine the chemical composition of the LBE. It was determined that there was more iron content in the LBE than could be explained by the experiment. It was theorized that the additional iron came from point defects in the oxide layer of the stainless steel vessel used for testing. This was rather surprising and annoying to find in terms of a corrosion study. You do not want to hear that the pipe intended to carry LBE for cooling in a nuclear reactor is slowly dissolving away. However, it did indicate to Dr. Johnson that other particles should also be able to be suspended this way, possibly providing a new catalyst delivery method. Further it led to the decision to conduct our experiments in quartz tubes to remove any chance of contamination via this phenomenon.

The three zone furnace used in the final reactor design allows us to set up a temperature gradient across the liquid metal support, the resulting convective loop coupled with the turbulence caused by the feed gas bubbling through the support keeps the particles moving. The catalyst will dissolve in the higher temperature bottom zone and begin to rise toward the lower temperature zone at the top of the liquid metal column where it tends to precipitate out of solution and starts fall back toward the higher temperature zone, thus regenerating the particle surface.

The suspension of the catalytic particles in the liquid metal support also plays an important role in our desire to produce carbon nanotubes. As will be discussed in the next section, CNTs require a catalyst as a starting point for the tubes to form. Here again

the transition metals, particularly the ones used in this experiment, are commonly used as catalysts for this process. We theorize that if the proper size catalyst particle (5-10 nm) can be generated, in-situ growth of nanotubes is possible. Further being much less dense they should collect or possibly be expelled at the top of the liquid metal column; again this will be further explored in the next section.

1.4 Carbon Nanotubes

Carbon nanotubes (CNTs) have recently become a hot topic in many research circles. This is due to the unique properties exhibited by CNTs, most notable being:

- CNTs exhibit extremely high thermal conductivity in the axial direction, in excess of 3000 (W/m K), yet exhibit very good insulating properties laterally to the tube axis.

- Exceptional mechanical strength in the axial direction, meaning high tensile strength and elastic modulus. Almost all of the literature available is in agreement that CNTs are the strongest and stiffest materials axially yet discovered.

- CNTs can be either metallic (conducting) or semi-conducting in their electrical behavior. Their conductivity is a function of the degree of twist, as well as the diameter of thee tube. Single-walled nanotubes are the most likely candidate for miniaturizing electronics beyond the micro electromechanical scale currently used in electronics.

- CNTs have a very large surface making them highly absorbent. Of great interest is their ability to trap hydrogen, thus they are of interest for use in certain ultra high purity filtration applications and battery anodes.

CNTs are allotropes of carbon with a cylindrical nanostructure. Allotropes are different structural modifications of an element; the atoms of the element are bonded together in a specific manner. Nanotubes are members of the fullerene structural family, which also includes the buckyballs. A nanotube is a hollow structure with the walls formed by one-atom-thick sheets of carbon, called graphene. These sheets are rolled at specific and discrete angles. The combination of the rolling angle (chiral) and radius decides the nanotube properties; for example, whether the individual nanotube is a metal or semiconductor. CNTs are classified as single wall or multi-wall, representations of which can be seen in Figures 1.2A and 1.2B.
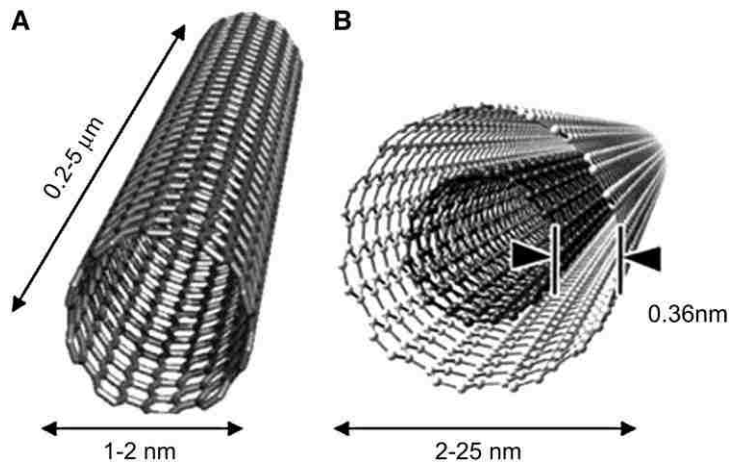
Figure 1.2A), B) Conceptual diagram of nanotubes [11].

(A) single-walled carbon nanotube (SWCNT) and (B) multi-walled carbon nanotube (MWCNT).

SWCNTs occur mainly in thick bundles, where they are combined by van der Waals attractions, much like spaghetti strands do if not stirred when cooking. This bundling effect can easily be seen in Figures 1.3A and 1.3B.
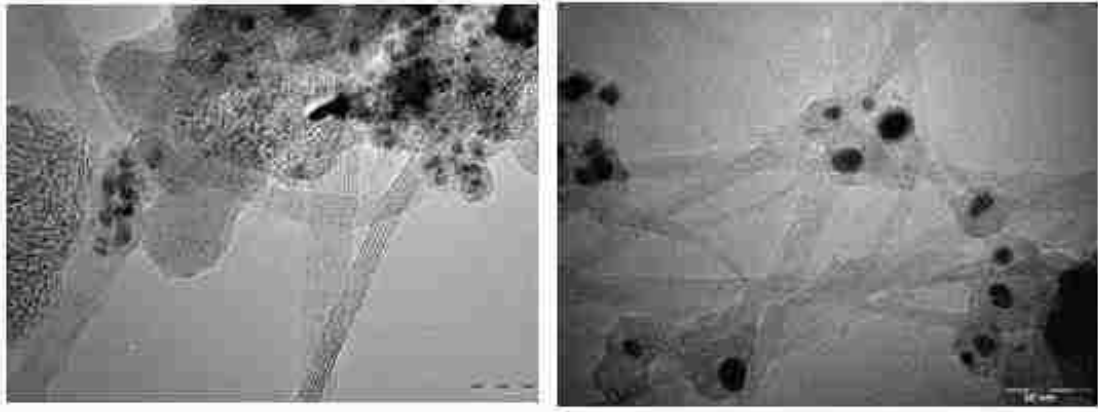
A) marker 20 nm   B) marker 50 nm.

Figure 1.3A), B) TEM image of the SWCNTs bundles [12].

It has been known for some time that carbon filaments may be produced by pyrolysis of hydrocarbons. These filaments are typically less than 0.5 μm in diameter and exhibit a "vermicular" (curled) structure. They generally grow on iron subgroup metal catalysts (Ni, Co, Fe, and Cr) where they are formed by catalytic decomposition of the hydrocarbons on metal particles [13]. SWCNTs are produced using a variety of methods, such as thermal chemical vapor deposition (CVD), laser ablation, catalytic chemical vapor deposition (CCVD), plasma enhanced chemical vapor deposition (PECVD) or arc discharge.

Much of the current work on CNTs has focused on their electrical properties. Many researchers envision using them in nano-scale electronic devices such as nano-wires, electron emitters, transistors, and even computer chips [14]. However, producing suitable nanotubes for these types of uses has proved to be quite difficult. As was mentioned the electrical properties are highly dependent on tube geometry, as such consistency is paramount. Although some lab scale devices have been demonstrated, there is currently no commercially viable process available. Further, due to surface

contamination by amorphous carbon and oxidation issues several purification steps are generally required to produce nanotubes with the correct properties. Finally, there is the problem of scale, due to the extremely small size of nanotubes completely new methods and tools have had to be developed. One particularly challenging issue is in-situ quality control, catching and examining a random sample during the process.

CNTs produced for their mechanical properties have enjoyed greater success. Research in the biomedical field has shown several promising uses for CNTs. In one application Aliev; et al. developed an artificial muscle made from carbon nanotubes [15].

In a totally different direction CNTs have become increasingly attractive for use in composite materials. Bulk carbon nanotubes have already been used as composite fibers in polymers to improve the mechanical, thermal and electrical properties of the bulk product. One such example of the use of bulk nanotubes, which is a mass of rather unorganized fragments of nanotubes, is Easton-Bell Sports, Inc. They have been in partnership with Zyvex Performance Materials, using CNT technology in a number of their bicycle components—including flat and riser handlebars, cranks, forks, seat posts, stems, and aero bars for racing cycles. Because of the carbon nanotubes superior mechanical properties, many structures have been proposed ranging from everyday items like clothes and sports gear to combat jackets and space elevators [16].

Our interest in CNTs lies in two areas, 1) we also believe CNTs produced in bulk form will be highly utilized in composite materials, and 2) CNTs have very high surface area, giving unique absorption properties. They are particularly good at trapping gas molecules, especially hydrogen. This makes them potentially very useful in fuel cells and energy storage applications, for which hydrogen is often a death sentence. This high

surface area and extremely small size also shows great potential for use as a filter media or permeable membrane.

Although it follows that a uniform nanotube will exhibit superior mechanical properties, this is not as critical for our intended application. We believe the use of free floating catalyst particle will tend to cause our tubes to grow in a more serpentine fashion much like the ones shown in figure 3A), B). Additionally, it is possible for tube growth in multiple directions from a single catalytic particle, thus they should be able to inter connect forming something similar to steel wool kitchen scrubber.

CHAPTER 2 INITIAL TESTING PHASE

As was mentioned in the introduction the work described in this paper has been conducted as a "back of the bench" working unfunded and with a very limited budget. As a result, the system is made up of existing assets that have been repurposed to fit the needs of this experiment, as well as several custom built components that were fabricated in the UNLV Physics and Mechanical Engineering machine shops. After discussions with Dr. Johnson it was decided that the minimum system requirements would include:

- Furnace with containment vessel to house process
- Mass flow controller for feed gas/ethanol delivery
- Quartz tube (one end closed) for lead alloy containment
- Quartz tube (one end closed) for submerged thermocouple
- Quartz tube (open on both ends) for gas delivery in molten lead alloy
- UHV system with mass spectrometer for determination of exit gas composition

2.1 Bench Tests

For the initial testing phase, lead bismuth eutectic (LBE) was chosen as the liquid metal support for the catalyst. The reasoning for this was twofold; as a eutectic LBE has a very low melting temperature (123.5°C) compared to pure lead (327.5°C) and we had access to approximately 35lbs left over from previous work. One concern in using LBE is expansion during cooling, Glasbrenner et al. (2005) showed that LBE allowed to freeze in a glass tube caused the vessel to crack; additionally our testing showed similar results in quartz test tubes [17]. Since it was decided that quartz tube would be used to contain the liquid metal, cracking of the process tube was a real possibility in the event of failure of the furnace allowing solidification of the LBE.

2.2 Vertical Test Setup

Figure 2.1 shows the tube furnace and containment vessel utilized during initial testing. The furnace is a 1200 W single zone unit with a maximum operating temperature of 1200 °C; however the containment vessel is made of stainless steel limiting the maximum to around 800 °C. An off the self compression fitting with a Viton® gasket is used to hold a 50.8 mm (2 in.) diameter quartz test tube. A cap with a 6.35 mm (1/4 in.) compression fitting to hold the quartz gas feed and fixed exhaust outlet was fitted to the top of the process tube, thus creating gas tight fit.

Figure 2.1 Vertical LMR test reactor

Two additional groups of components were required to complete the system. Feedstock is delivered to the inlet side of the LMR via a mass flow valve and multi channel gas controller. A compressed mixture of 98% argon + 2% hydrogen is first bubbled through the liquid metal column to remove oxides. Compressed ultra high purity (99.999%) argon is used as a carrier gas which is bubbled through standard reagent ethanol for delivery to the system. Standard T size bottles feed a MKS 1197 mass flow valve which is controlled by a MKS 647C multi-channel gas controller. The controlled

flow is then directed into the LMR in the hydrogen mix case. In the case of the UHP argon, it is first bubbled through the alcohol and then into the LMR. Figure 2.2 shows the basic process path for the system.
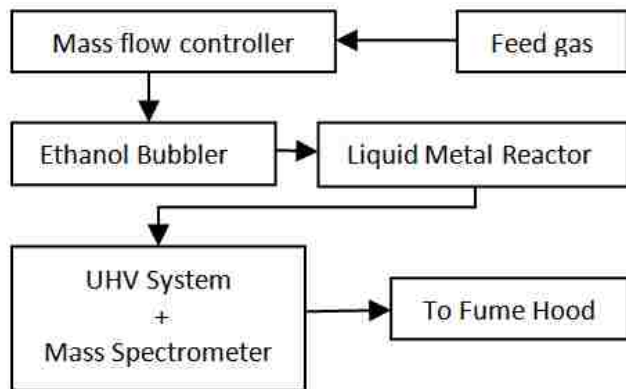
Figure 2.2 Process path

The remaining components are on the outlet side of the LMR and are used to sample the reaction gases. These components include:

1) High vacuum pump system

   a) An Edwards PicoDry self contained pump cart was used for initial testing and the first two LBE tests. This system can achieve vacuum to 1x10-7 Torr which is sufficient for the analyzer we used (many analysis techniques require vacuum 2 or more magnitudes better).

2) A vacuum leak valve

   a) This allows a sample of the output gas into the vacuum chamber in a finely controlled manner.

3) A mass spectrometer, a SRS residual gas analyzer (RGA 300)

   a) This is attached to the vacuum system and is used to analyze the components of the outlet gas.

4) Control System Software (RGA version 3.210.002)

   a) The analysis and data acquisition is controlled by a software package on a PC.

Figure 6 shows the complete initial testing setup.
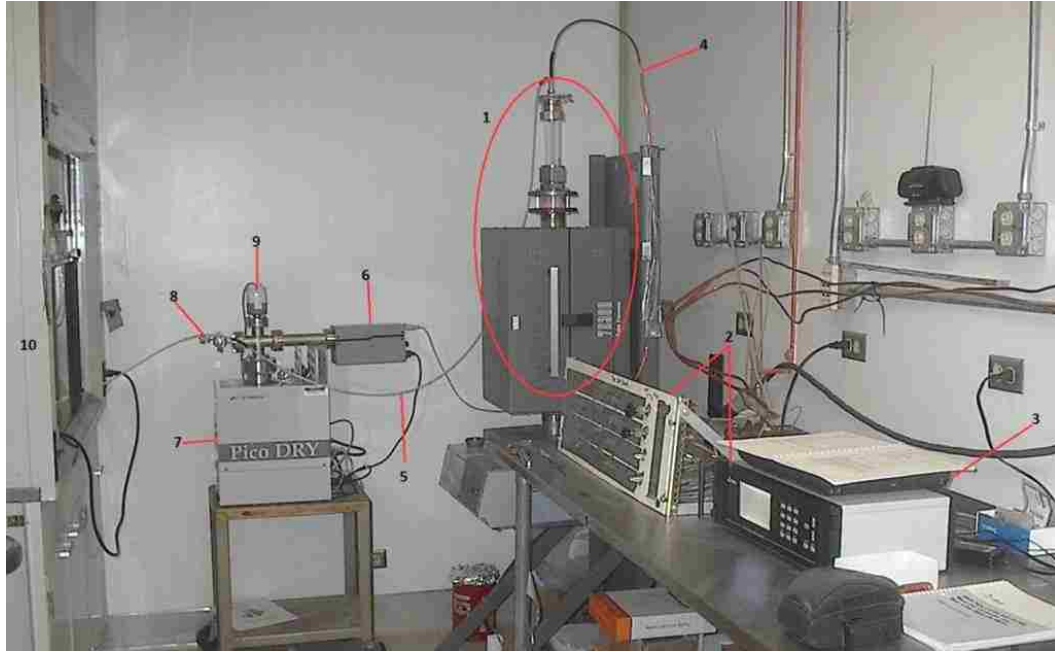
Figure 2.3 Initial test system components

1) LMR (furnace, containment vessel, and process tube) 2) Mass Flow Controller and gas controller 3) Laptop computer 4) Feed stock delivery (ethanol bubbler hidden) tube 5) Process gas outlet 6) SRS RGA200 Mass Spectrometer 7) High vacuum pump system 8) Sampling valve 9) Pressure gauge 10) Exhaust hood

2.3 Results

Initial testing has shown that the feedstock delivery system works well. The oxidation layer present on top of the LBE column was effectively removed using the argon-hydrogen mix. Further it was determined a minimum flow rate of 15.0 sccm was required to achieve a steady bubbling rate through the LBE column. Additionally, the product gas sampling and analysis components were also found to work as expected. The mass spectrometer was easily able to determine the differences in the argon, argon-hydrogen mix, and argon carrier gas bubbled through ethanol. Although hydrogen production was not observed, possibly due to ethanol saturation of the sampling valve, a

17

heavy carbon particulate build up was observed on the process tube indicating a low temperature catalytic reaction.

However, initial testing also revealed several problems with the vertical configuration. The first problem noted was that removing the process tube containing in excess of 20lbs. of LBE from the furnace at a temperature in excess of 150°C would be difficult and dangerous. The only option in this configuration was to allow the LBE to freeze in the process tube, thus a new process tube would be required each time the system is shut down.

The second problem noted was the contact time between the bubble and LBE was not long enough to allow decomposition of the ethanol. The resulting saturated ethanol vapors then began condensing when the temperature of the process gas dropped below the vaporization temperature of ethanol. It is also very probable the condensate includes condensed water vapor produced by the lower temperature catalytic reaction.

The final problem encountered was lead contamination in the carbon particulate. Since one of the goals of this research is a less harmful form of carbon by-product, the production of lead laced bricks would not be in our best interest.

2.4 Conclusions

Initial testing has shown the reactor section of the test apparatus must be redesigned to 1) increase contact time between feedstock and liquid metal support, 2) heat the path between process tube and analysis sampling valve above the vapor point of ethanol to address condensation issues, 3) include a temperature gradient in the liquid metal column as necessary to control lead contamination of the carbon particulate due to lead vapor pressure issues encountered at temperatures above 650 °C.

CHAPTER 3 LBE SUPPORT TESTING

3.1 System Design Changes

The feedstock delivery and high vacuum analysis portions of the test setup

performed as expected and required no major modifications as was noted in Chapter 2. It

should be mentioned however that during subsequent testing of the 2nd generation system

design our PicoDry high vacuum cart suffered a turbo pump failure. Though this is not

uncommon in this type of testing, repair is both costly and time consuming. As such, a

replacement cart was built using various independent components again made available

by Dr. Johnson. After the pump cart was replaced the plumbing between the process tube

and the leak valve was wrapped in heat tape to address condensation issues. A type K

thermocouple was placed under the tape and then the tape was covered in foil to help

retain the heat. This section of plumbing and the leak valve are now heated to ~ 100 °C

during system operation.

Having no prior experience with this type of equipment this required development

of a new skill set. High vacuum systems require a great deal of care when being setup; a

single finger print can cause serious problems. (Here again I have to thank Dr. Johnson

for his patience during this learning process and allowing me great latitude in learning

how to use some rather expensive equipment).

Major changes were made to the reactor section of the design. The vertical single

zone furnace is replaced with a three zone 5.1 kW horizontal tube furnace. This change

had been anticipated from the start. One of the major goals of this project was to test the

non-isothermal behavior of the catalysts and liquid metal support. Figure 3.1 shows the

furnace setting in a rack built to allow the entire furnace to be rotated up to 45°. Initial

testing determined that a 15° tilt gives a bubble contact time of approximately 1.5

seconds when operating at 300 °C isothermal. As the temperature rises the density of the LBE goes down, thus the bubbles speed up and the contact time shortens to about 1.25 seconds at 700 °C.

Figure 3.1 Three zone horizontal furnace

With this configuration the top of the lead column can be as much as 100 °C cooler than the bottom third, thus given some control to the vapor pressure issues encountered at higher temperatures. In addition to increased contact time and a controllable temperature gradient; this configuration safely allows for the liquid metal support to be poured off at the end of a run, saving the process tube for reuse.

3.2 Generation 2 Experimental Setup

Figure 3.2 shows the process path for the second generation design. Although the actual reactor design has been updated, and a new vacuum pump cart is being used; the overall process path has not been altered. From a physical stand point this simply required some alterations to the plumbing. The process gas delivery components have not changed from the initial design. The outlet side of the process has seen the

introduction of new vacuum pumping hardware, however the same product gas sampling and analysis equipment is utilized from the inital test apperatus.

1. Gas Cylinders
   a) Process Carrier Gas (argon)
   b) Purge Gas (98%Ar+2%H$_2$)
2. Mass Flow Controller
3. Ethanol Bubbler
4. 3 Zone 5.1kW Tube Furnace
5. 76.2 mm (3 in.) Quartz Containment Tube
6. 25.4 mm (1 in.) Quartz Process Tube for Lead Alloy
7. Stainless steel encased K Type Thermocouple inside 4 mm quartz tube w/end closed.
8. 4 mm quartz tube w/end open (process gas bubbler).
9. UHV System with SRS Mass Spectrometer
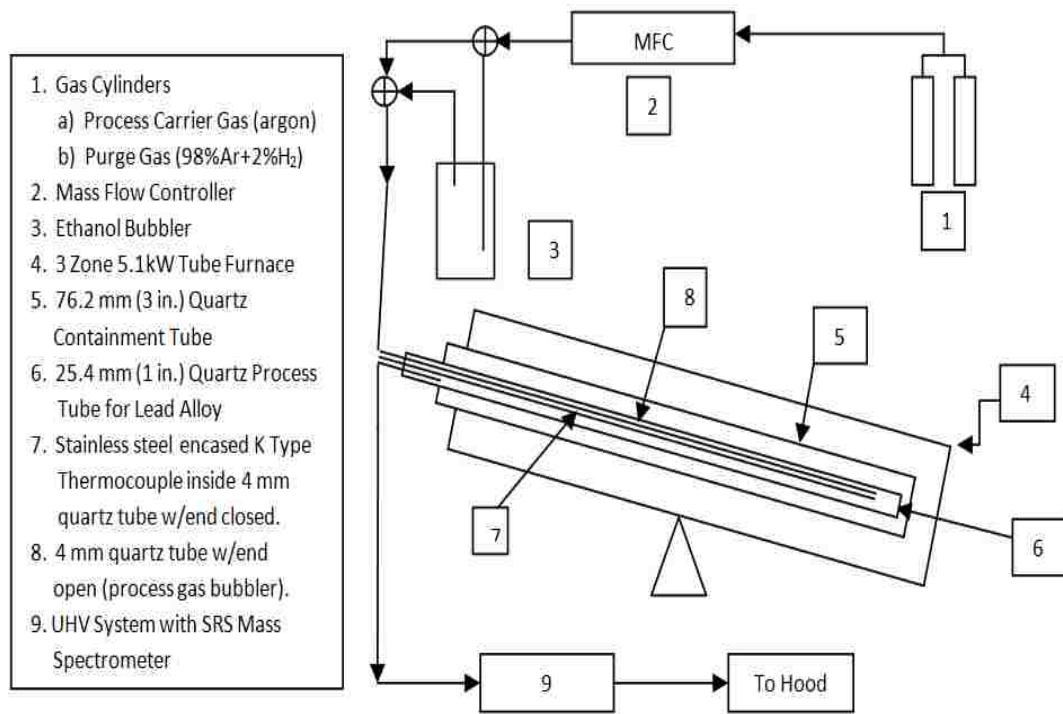
Figure 3.2 Generation 2 process path schematic

Figure 3.3 shows the reconfigured vacuum system. From the picture it is easy to see the components are larger in this system. As a result, this system is capable of reaching 8×10^{-9} Torr, which is on the order of 1.5 magnitudes better than the PicoDry pump cart originally used. Additionally, all of the plumbing was replaced with copper tube. The tubing is wrapped with heating tape and then covered in foil. The same process is used on the leak valve and analysis chamber. Everything between the outlet of process tube up to the sample valve is heated to 110 °C which is above the boiling point of ethanol and water, 78 °C and 100 °C respectively.

Figure 3.4 shows the three sections of the furnace, as well as the quartz containment and process tubes. A 76.2 mm (3 in.) quartz containment tube holds the

25.4 mm (1 in.) quartz process tube using a compression fitting with a Teflon gasket. Approximately 61cm (24in.) of the quartz process tube is heated by three thermostatically controlled zones.
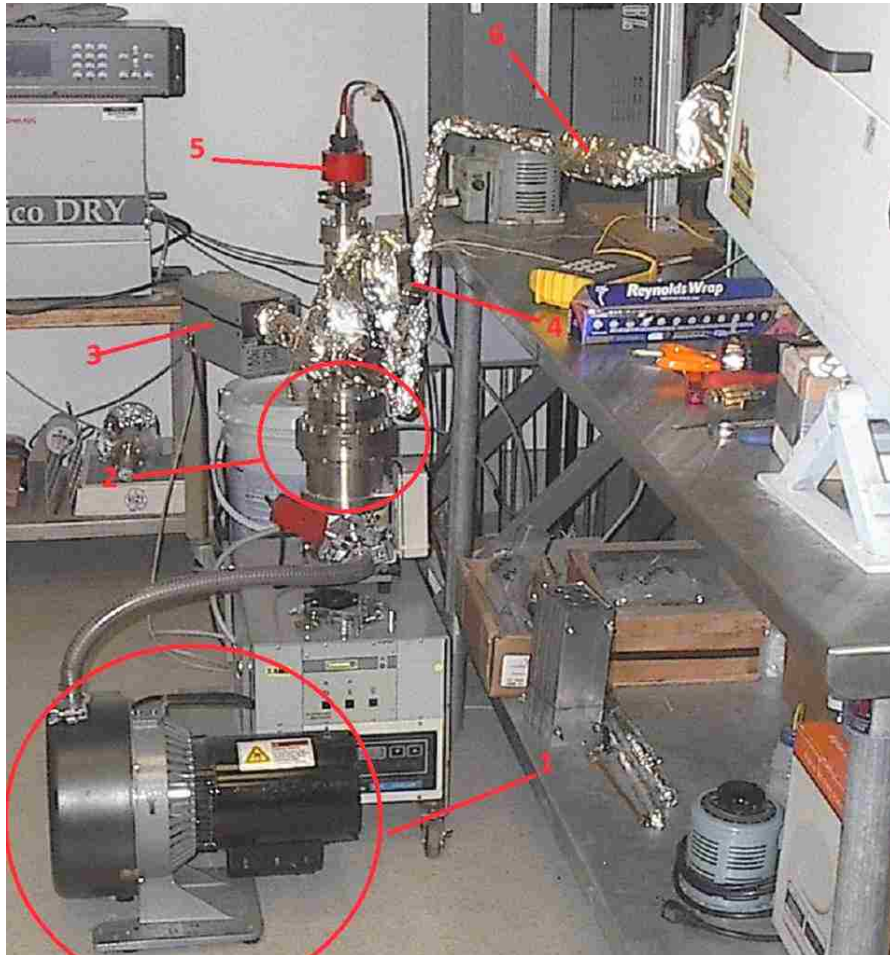
Figure 3.3 Replacement high vacuum system and analyzer
1) Backing Pump 2) Turbo Pump 3) SRS RGA200 Mass Spectrometer
4) Sampling valve 5) Pressure gauge 6) Heat tape under foil (filter section)

The volume of the process tube was computed and based on the density of the LBE. It was determined that 2.4 kg (85oz.) was needed to provide the maximum length column of liquid metal support. Finally, the liquid metal support was cast into slugs and inserted into the process tube. Figure 3.5 shows the mold for casting, the cast slugs being weighed and inserted, and the liquid metal support after heating.

Figure 3.4 Containment tube with process tube (gen 2)

Figure 3.5 Liquid metal support preparations

1) Mold 2) LBE slugs 3) inserting slug in process tube 4) LBE in liquid state

In Figure 3.6 the process gas inlet and outlet pathways can be seen. From the sampling leak valve the process gas is sent to a condensate trap, located in the fume hood, and then bubbled through mineral oil to trap any remaining particulate matter (Figure 13).
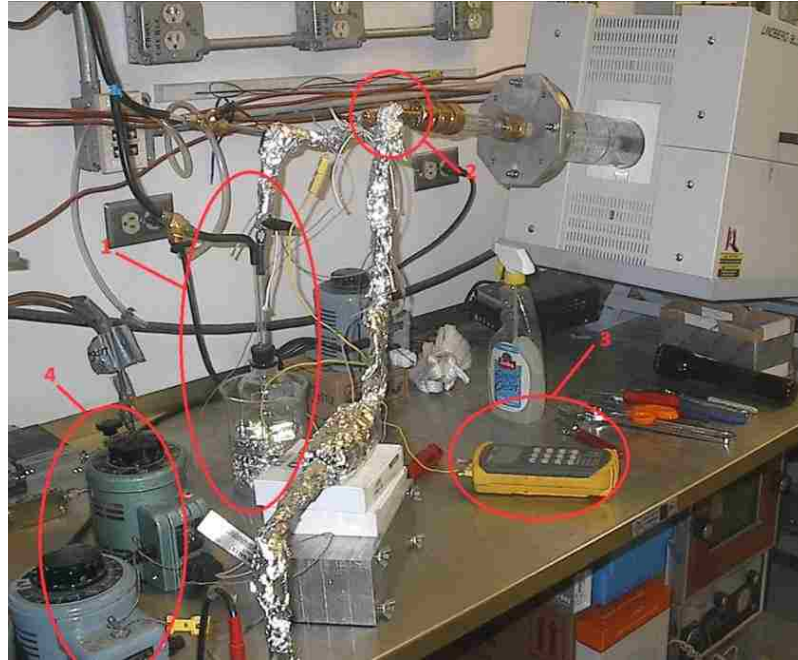
Figure 3.6 Process gas pathway

1) Ethanol bubbler 2) a) gas inlet tube, b) thermo couple tube, c) process gas outlet
3) thermo-couple reader 4) heat tape power source

Figure 3.7 Condensate and particulate trap

3.3 LBE Background

Lead-Bismuth Eutectic or LBE is a eutectic alloy of lead (44.5%) and bismuth (55.5%), and has been used as a coolant in some nuclear reactors. LBE was most notably used as a coolant in the nuclear reactors of Soviet Alfa-class submarines. A eutectic system is a mixture of chemical compounds or elements that has a single chemical composition that solidifies at a lower temperature than any other composition. LBE has a melting point of 123.5 °C (254.3 °F) and a boiling point of 1670 °C (3038 °F).

A study by Glasbrenner et al. (2005) mentions the possibility of interactions between steels and LBE, which might lead to liquid metal corrosion or liquid metal embrittlement (LME) [17]. This phenomenon also was the focus of the unpublished research conducted by Dr. Loewen (section 1.3) and led to the catalyst support system tested in this work.

3.4 Catalyst Information

The catalyst was introduced to the system in the form of a wire sample wrapped around the outside of the quartz tube used to house the thermo-couple as shown in Figure 3.8.

Figure 3.8 Nickel catalyst ready for insertion into system

The wire samples used were laboratory grade, 99.9% purity or greater. The samples were handled with latex gloves to avoid any surface contamination. As mentioned in the discussion of catalysts, nickel and cobalt are traditional choices. Our system used 30 cm of 99.9% pure nickel wire 0.25 mm in diameter and 10 cm of 99.995% pure cobalt wire 1.0 mm in diameter. The cobalt was used more sparingly due to the cost. Additionally 60 cm of 99.99% iron wire 1.0 mm in diameter was also tested. The iron was found to be the least soluble; when the thermo-couple tube was removed at the end of the experiment, traces of the coiled wire were still visible. None of the original wire sample was visible when the thermo-couple tube was removed from the nickel and cobalt runs.

3.5 Experimental Procedure

The furnace is set to melt the liquid metal support isothermally, at 300 °C for LBE and 400 °C for lead. The 4 mm quartz thermo-couple and bubbler tube are inserted into the molten support. Figure 3.9 shows the process tube cap with fittings to hold the 4 mm tubes and exit port for the process gases.
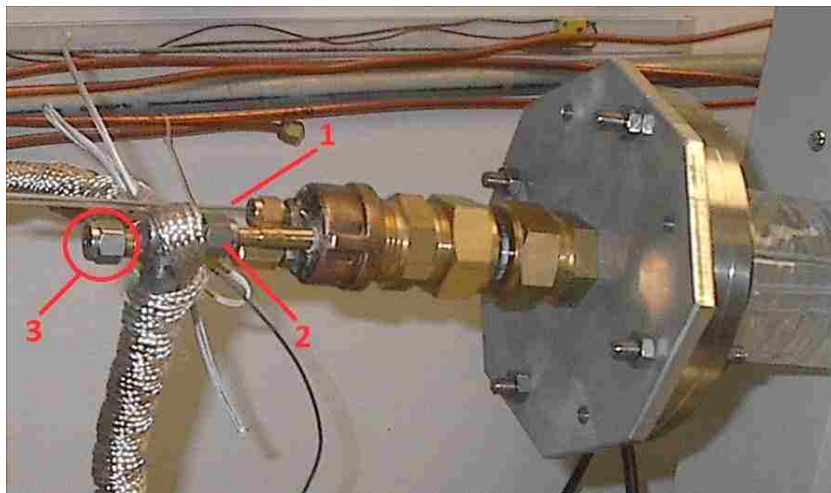

Figure 3.9 Process tube cap

1) Thermo-couple tube 2) process gas outlet 3) process gas inlet

Special notice of the circled cap marked 3 should be taken; this was used as the inlet for direct injection of ethanol into the system and is discussed in the other results section. After tightening of all the fittings the Ar-H$_2$ gas flow is started and the system checked for leaks. Once the system reaches equilibrium, a steady bubbling rate can be observed in the mineral oil trap and is the basic indicator the system is running normally. The liquid metal column has a small oxide layer at the exposed surface once melted. Allowing the Ar-H$_2$ gas mixture to bubble through the column for up to 24 hrs efficiently removes this layer leaving the shiny liquid seen in Figure 3.5.

Once the oxide has been removed the gas flow is switched to the ultra high purity argon gas bubbled through ethanol. The mass spectrometer (residual gas analyzer) is then initialized and the background spectrum of the chamber is taken. While the transition to the generation 2 reactor was made, the RGA was sent to the factory for service and calibration. The following excerpt from the SRS RGA 300 operations manual explains the systems basic operating principles:

> Complete characterization of a vacuum environment requires the detection of all the component gases present, as well as measurement of the total pressure. The instruments used for this purpose are called Residual Gas Analyzers or Partial Pressure Analyzers. A Residual Gas Analyzer (RGA) is mass spectrometer of small physical dimensions that can be connected directly to a vacuum system and whose function is to analyze the gases inside the vacuum chamber. The principle of operation is the same for all RGA instruments: A small fraction of the gas molecules are ionized (positive ions), and the resulting ions are separated, detected and measured according to their molecular masses. RGA's are widely used to quickly identify the different molecules present in a residual gas environment and, when properly calibrated, can be used to determine the concentrations or absolute partial pressures of the components of a gas mixture. The first step in the spectral analysis process is to correctly identify the mass-to-charge ratio of all the peaks in the mass spectrum. A well calibrated mass scale is essential to this task. See the RGA Tuning Chapter for a detailed description of the mass scale calibration procedure. Once all the peaks have been labeled, the next step is to identify the residual gases that have produced the spectrum. Knowledge

of the recent history of your system may provide very valuable clues as to the possible gases that may be residuals in the vacuum chamber. A familiarity with the standard spectra of commonly expected gases will generally help to determine the major and minor components in the system. Any peak in the spectrum may consist of contributions from molecular ions and/or fragment ions, or multiply ionized species. The qualitative spectral analysis is completed when all the peaks in the spectrum have been "uniquely assigned" to the components of a gas mixture, in complete agreement with the known fragmentation patterns of the components [18].

Figure 3.10 shows the first background spectrum taken after reinstallation and pump down of system. These data were sent to SRS and approved as operating properly. It is important to note here that there is simply no way to achieve a perfect vacuum, thus we do not see a straight line at zero in the graph. Vacuum is a term used by the sciences to indicate a lack of matter, meaning the goal is to remove as many individual atoms as possible. The four major peaks in the graph are commonly seen in a well operating vacuum system.
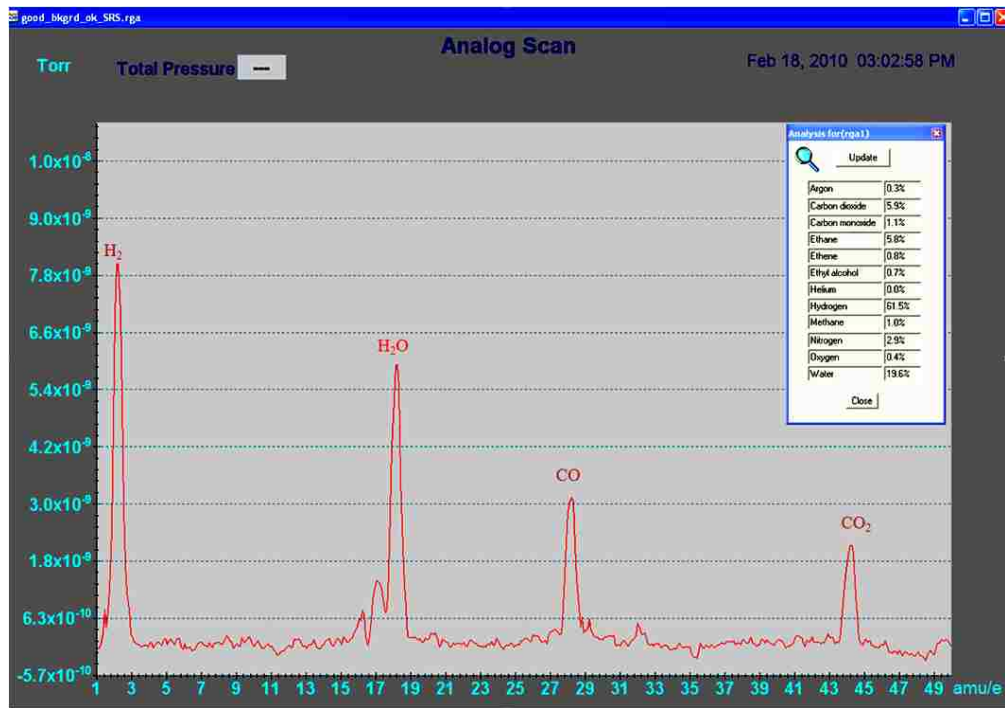

Figure 3.10 Typical system background spectra

28

The peak at 18 indicates water (H_2O) which likes to adhere to the walls of the sample chamber. This peak can be dramatically decreased by raising the temperature of the heat tape to between 150-200 °C for several hours. This is referred to as "baking out the system" and is commonly repeated during experimentation to remove excess water that develops during sampling and analysis.

The peaks at 28 and 44 are CO and CO_2 respectively. These two compounds are present due to the reaction between the hot filament used for ionization and water present in the system. The filament contributes the carbon atoms of the water molecule yields the oxygen atom with hydrogen left over. Here again "baking out" the system will help lower these concentrations.

Finally we see a peak at 2; this is the dreaded H_2, the scourge of every vacuum system. Being the smallest of all the elements, it will always be present. In fact hydrogen is so small it can actually migrate through the stainless steel walls of the system over time.

For simplicity the graph shows the presence of an element or compound based on the molecular mass of the element or compound. This scale can cause problems in the fact that N_2 (2x14) and CO (12+16) both show up as 28. The analysis software has a library function that helps indicate which of the possibilities is more likely to be present based on the rest of the compounds and elements present. A certain amount of common sense also helps, since the carrier gas is very pure and no nitrogen is expected to be produced and CO is expected to be present it is reasonable to assume the peak at 28 is CO.

At this point the system is considered to be in operational mode. The furnace is then adjusted so that a temperature gradient is established. Typically the temperature

was set so the top most zone was between 75-100 °C lower than the bottom zone, thus the center zone is generally at the mean temperature of the gradient. The first gradient was set so the zones were at (400, 450, 500) °C respectively. Although many different incremental changes were tried as the temperature of the system was raised, at least one reading was taken at every 50 °C rise of the middle zone. These data points being common to every run were then used to chart the data in Excel.

A total of eight runs in the generation 2 reactor are documented in the following sections. The first four runs were made using LBE as the liquid metal support, while the second four runs used 99.99% pure lead. The initial run in each support metal was performed catalyst free and would serve as the baseline. The baseline run was allowed to proceed until hydrogen and CO production both showed up in the spectroscopy, indicating the expected high temperature reaction has started. This reaction typically occurred between 650-700 °C in the non-catalyzed runs. This procedure was then repeated with each of the catalysts inserted into the system.

3.6 LBE Support Results

Figure 3.11 shows the initial spectrum results for the non-catalyzed LBE run. At this point a 100 °C temperature gradient was established, actual thermo-couple readings are incorporated in the file name which appears in the upper right hand corner of the graph. The major peak appears at 40, this as expected is argon (Ar^+), which is the carrier gas. Another peak at 20 also indicates argon, in this case (Ar^{2+}). The peaks of interest in this study are located as follows:

- Hydrogen (H_2) @ 2
- Carbon monoxide (CO) @ 28
- Carbon dioxide (CO_2) @ 44

30

Based on the molecular weight a peak would be expected at 46 indicating ethanol. Although there is a small peak at 46 the ethanol is actually represented as fragments at 26, 27, 29, and 31 as determined by the library function of the SRS software.
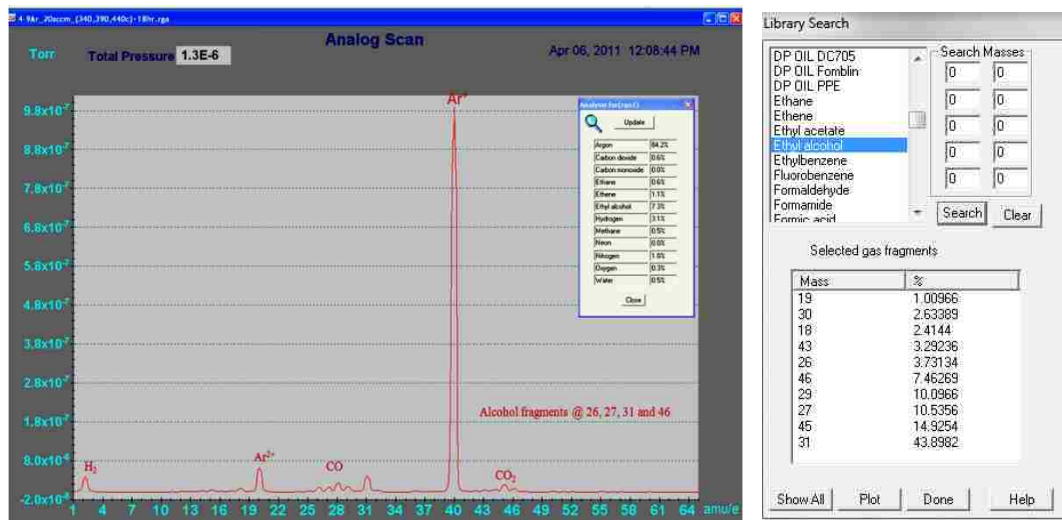

Figure 3.11 Initial spectra non catalyzed LBE 390 °C mean with library function

Figure 3.12 shows the spectra for the non catalyzed reaction at 700 °C. H_2 and CO production has increased and the alcohol fragments are disappearing.
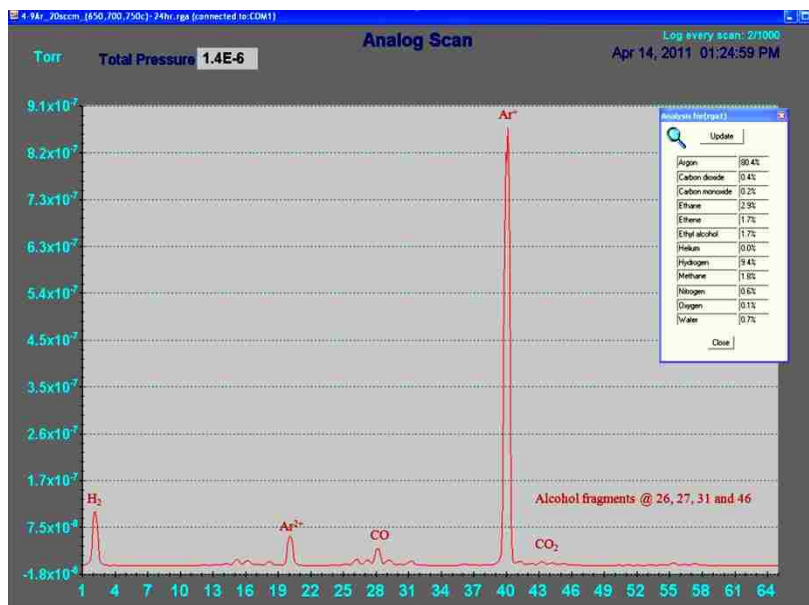

Figure 3.12 Spectra non catalyzed LBE 700 °C mean

Finally, Figure 3.13 shows the spectra with the system mean temperature @ 800

°C. Here significant H_2 production and increased CO production can be seen.
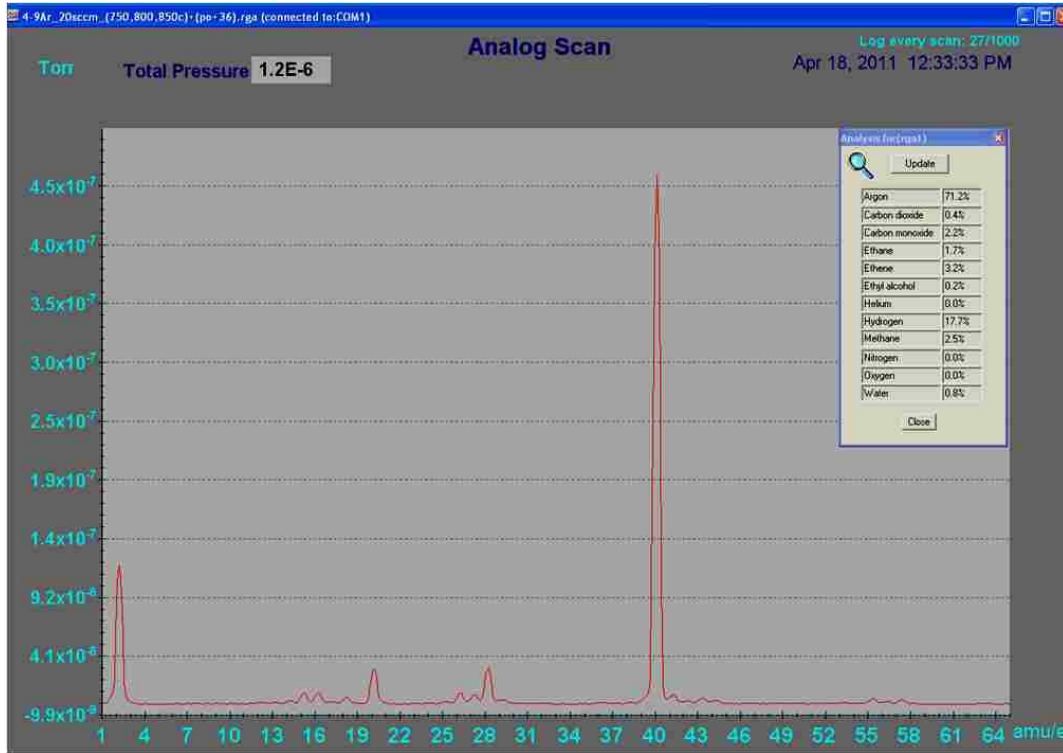
Figure 3.13 Spectra non catalyzed LBE 800 °C mean

The SRS software has a built in analysis mode (the small inset window) that allows the user to track specific elements and compounds. Again the description of the operating principle comes directly from the SRS user's manual:

Spectrum Analysis description

This utility provides the user with immediate analysis of residual gas based on a complete histogram or analog scan. Using a matrix inversion technique, the composition of the residual gas is analyzed and the best approximation to its composition is given in either pressure units or percentages. The user can enable up to 12 common gases for analysis [18].

In Figure 3.14 the gas composition of the process outlet gases is shown in the percentage mode. As can easily be seen, this mode provides quantitative indication of what is actually being produced at any given time.
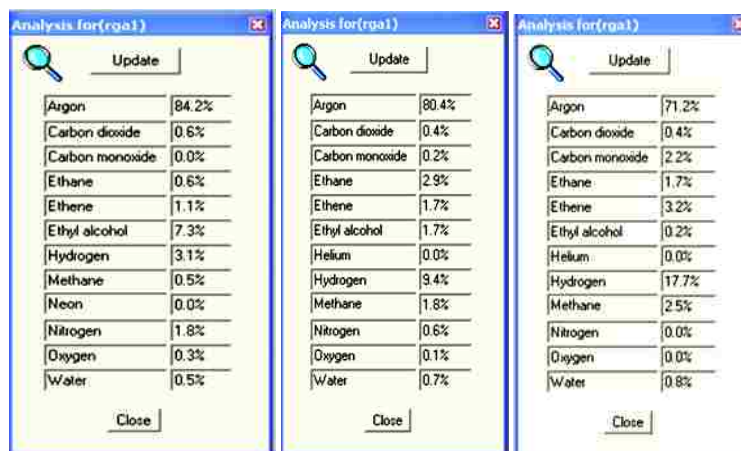
Figure 3.14 Gas % @ 390, 700, and 800 °C mean

While the analysis mode provides a good snapshot of what is going on during normal operation of the reactor system, the data still must also be tracked over the entire process. For this purpose the data were transferred to an MS Excel spread sheet and graphs generated. Since this study was predominately interested in hydrogen production and carbon sequestration only the trends of H_2, CO, CO_2, and ethanol were tracked.

Figure 3.15 Gas % at various temperatures no catalyst in LBE

Figure 3.15 graphically shows the onset of hydrogen production as the ethanol begins thermal decomposition. Additionally it should be noted that the onset of CO production occurs around 700 °C, a trend that would repeat in all eight test runs.

Once the onset of CO production is noted the system was generally backed down 25 °C and allowed to run for several days to several weeks. The experiment is then terminated and the system brought back t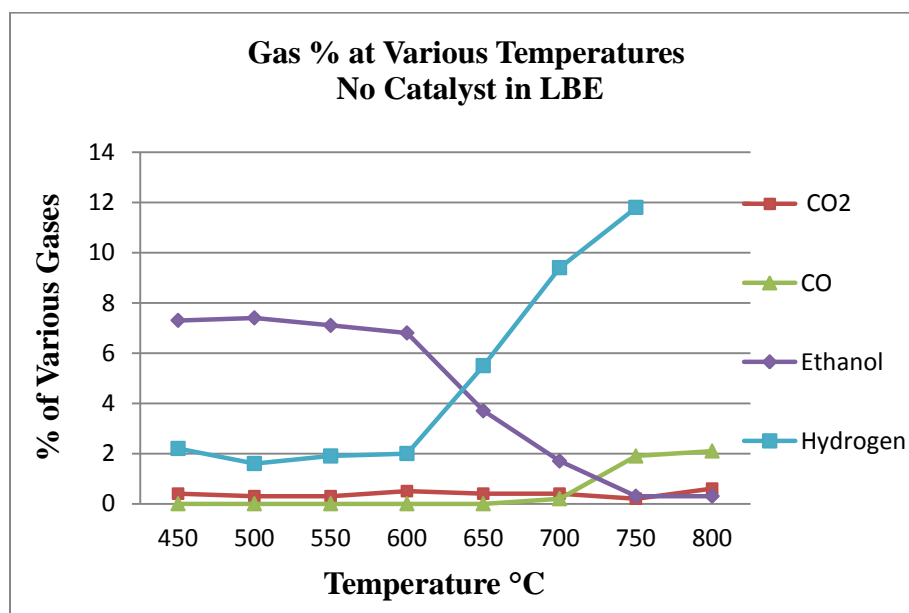o 300 °C (isothermal). Sample swabs are taken from the inside of the process tube for analysis in the TEM. The 4 mm tubes are removed from the process tube and the liquid metal support is then poured back into the slug mold for later reuse or examination. The entire process was then repeated with the addition of the catalyst using fresh liquid metal support. The data for each run are again collected and tabulated. Upon completion of the catalyzed runs a comparison of the hydrogen production was possible, the results of which can be seen in Figure 3.16.
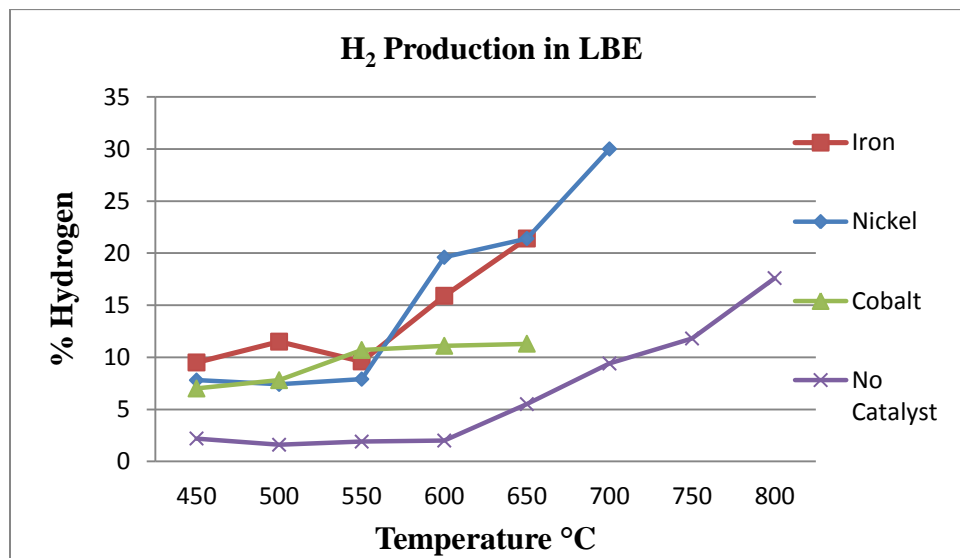

Figure 3.16 H$_2$ Production in LBE

As was hoped, to some degree, all of the catalyzed tests resulted in a lower temperature hydrogen producing reaction with no CO present as a byproduct. The first thing that should be noted from the graph is the higher background hydrogen in the

catalyzed reactions. The discussion on hydrogen production methods in Section 1.2 stated that many of the studies done have noted the fact that there are many simultaneous reactions with varying activation energies occurring during the decomposition process, and have been seen across a wide range of temperatures and conditions in most of the literature. The increase in background hydrogen indicates that the catalytic effect also has an effect on these simultaneous reactions. The data for the nickel and iron catalyzed runs show the onset of hydrogen production may begin as much as 100 °C earlier in the catalyzed reaction. In the case of the cobalt catalyst, increased production may begin as much a 150 °C earlier.

Although the production of hydrogen is observed to begin at lower temperatures in the catalyzed tests, there is no corresponding drop in the temperature seen where the production of CO is observed to start in the nickel and cobalt catalyzed runs. However production of CO starts around 50 °C earlier when iron is used as a catalyst. Figure 3.17 clearly shows a specific temperature range where each of the catalyzed reactions begin producing CO.
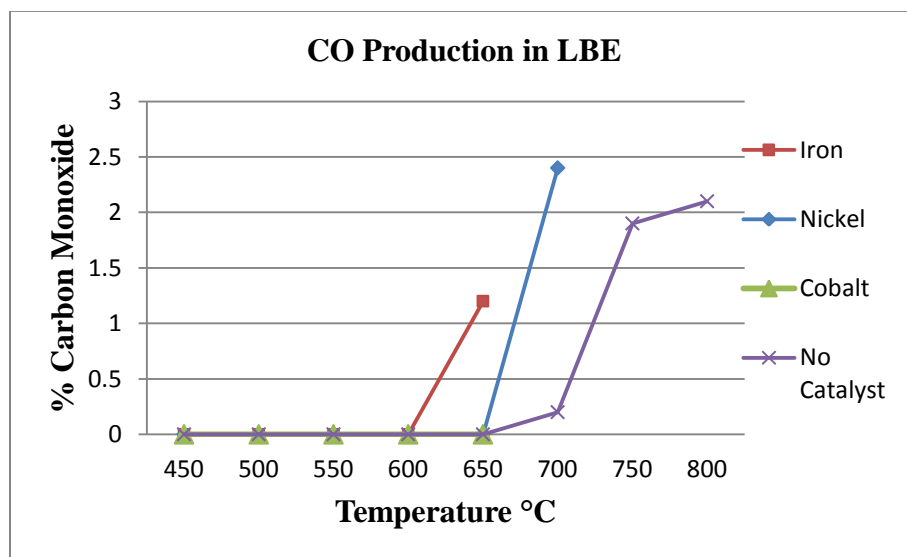

Figure 3.17 CO Production in LBE

Figure 3.18 shows that the production of methane (a component of the higher temperature thermal reaction) also begins at slightly lower temperatures in the catalyzed reactions.
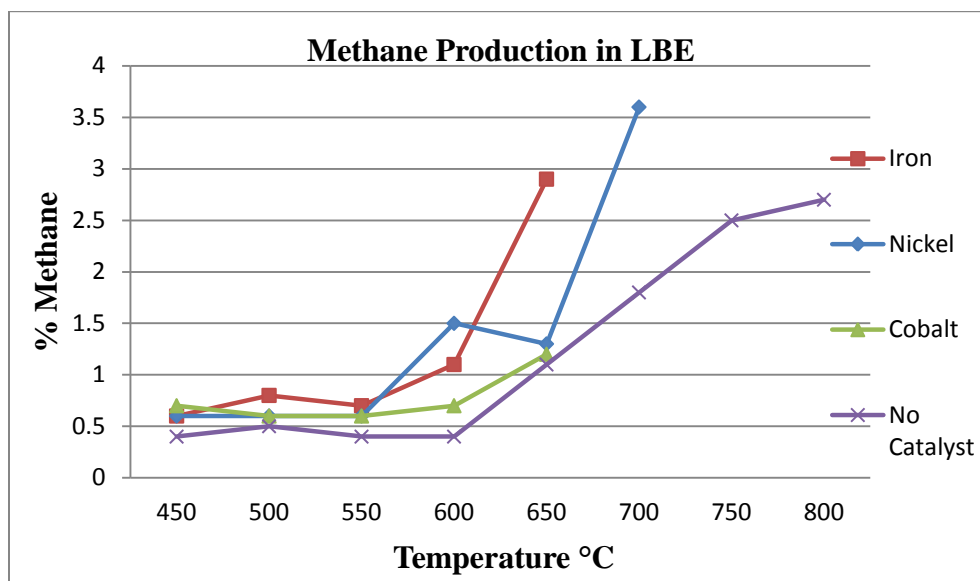
Figure 3.18 CH$_2$ Production in LBE

The discussion of catalysts in Section 1.3 mentions that using catalysts can change the speed of a reaction or allow for a more selective reaction. Proper selection of catalysts can lower the activation energy for certain reactions and not others. Table 3 illustrates how these selective changes can be charted and used to achieve a desired output. For this reason a great deal of time and money is invested in catalyst testing and preparation.

Table 3 Comparison of production increase onset temperatures

	Onset Temperature (°C) for different catalyst types				Approximate Temp. difference (°C)		
	Fe	Co	Ni	No Cat	Δ Fe	Δ Co	Δ Ni
CO	600-650	650-700	650-700	650-700	50	0	0
CH$_4$	550-600	600-650	550-600	600-650	50	0	50
H$_2$	550-600	500-550	550-600	600-650	50	100	50

The last parameter examined was the decomposition of the alcohol. Figure 3.19 shows the nickel and iron catalysts allow the reaction to decompose the available alcohol at a temperature below the onset of CO production, thus limiting the total possible production of hydrogen. Alternative delivery methods designed to increase the initial concentration of ethanol delivered to the system are discussed in the next chapter.
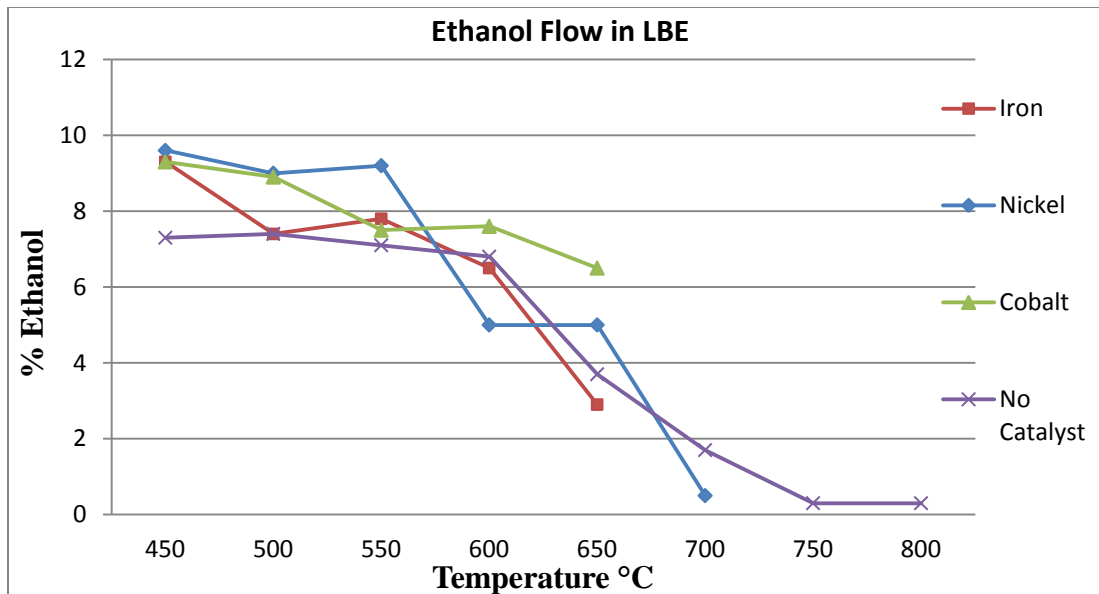
Figure 3.19 C_2H_5OH Production in LBE

3.7 Discussion of LBE Support Testing

It should be pointed out that the results presented in the previous section represent only initial testing, thus they are not conclusive. Instead these results indicate that the basic theory being tested, that a low temperature catalyzed reaction can produce hydrogen without CO gas as a byproduct is possible. These initial data have indicated specific temperature ranges for each catalyst that should be more extensively explored.

Design changes made to the second generation reactor successfully addressed problems encountered in the initial testing phase. The addition of heating tape has alleviated condensation build up between the top of the process tube and the sampling

valve. The use of the three zone furnace has allowed the development of a controllable temperature gradient, aiding in the circulation and regeneration of the catalyst. Although carbon samples taken from the process tube directly adjacent to the top of the liquid metal column still shows some support (LBE) contamination, samples taken further up the process tube show highly diminished amounts of contamination.

Further, spectra taken after several weeks of continuous operation shows no drop off in hydrogen production. This implies the novel concept for delivery and regeneration of the catalyst works adequately. This also implies further long term testing is needed to determine the operational lifetime of the catalyst. Based on the various production onset temperatures observed, the possibility exists that a combination of catalytic metals may further enhance the selectivity of the reactions.

From the stand-point of using a single catalyst, nickel was clearly the best performing in this round of testing. The nickel catalyst lowered the temperature that increased hydrogen production while keeping the temperature where CO production increases at the same level as the non catalyzed reaction. It is also apparent that the catalyzed reactions also increase production rates, here again the nickel catalyst showing the biggest increase. Additionally, in this round of testing an arbitrary amount of each catalyst was used, further testing is needed to determine both the minimum amount of catalyst material necessary to influence the reaction; as well as if there is a possibility of an over saturation condition being produced.

Overall the LBE support testing produced very satisfying results. Proof of concept was shown for the reactor setup, the catalytic reaction theory, as well as the catalyst delivery/regeneration concept. The data generated in the first round of testing

have provided some insight into which direction future work should proceed. It should be noted that chapter five examines the carbon formations resulting from this testing which are also of interest. This also has a bearing on the direction of future testing. Initial testing indicates a cobalt catalyst may produce exotic carbon formations such as nanotubes; however it was not a particularly good catalyst for increased hydrogen production

CHAPTER 4 LEAD SUPPORT TESTING

4.1 Lead Support Testing

After completion of the LBE support testing it was decided that the temperature range of interest was between 500-700 °C. Additionally, the LBE testing showed that recapturing the liquid metal support was safe at 400 °C, thus it was decided that lead could be tested as a support mechanism. For this phase of the testing 99.99% pure lead was used. The same experimental procedure used in the LBE support testing was followed for the lead runs. As before a non-catalyzed run was performed as a baseline and followed by the testing of the three catalysts.

4.2 Lead (Pb) Background

Lead is a main-group element in the carbon group with the symbol Pb (from Latin: *plumbum*) and atomic number 82. Lead has been commonly used for thousands of years because it is widespread, easy to extract and easy to work with. It is highly malleable and ductile as well as easy to smelt. The melting point of lead is 327.46 °C (621.43 °F) and a boiling point of 1749 °C (3180 °F).

4.3 Lead Support Results

Figure 4.1 shows the initial spectra of the non-catalyzed run performed with lead as the support. As expected the resulting data were very close to the run performed in LBE. The major exception being a slight rise in the ethanol percentage and the accompanying decrease in argon. This change is most probably due to the addition of a heating tape to the plumbing between the ethanol bubbler and the top of the process tube. About a 2% increase was noted, this topic will be explored more fully in the additional results section, where alternative delivery methods are discussed.
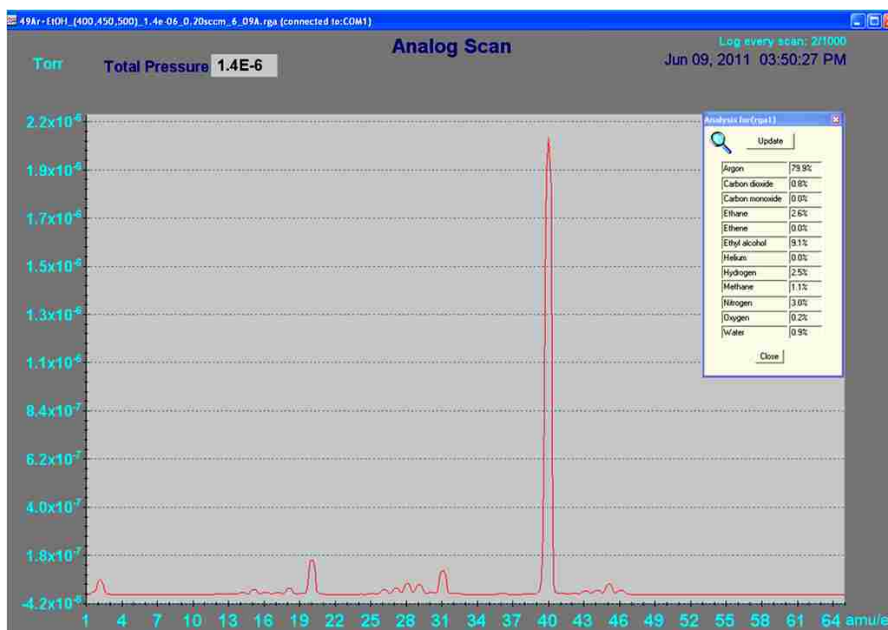
Figure 4.1 Initial spectra non catalyzed Pb 450 °C mean

The percentages of CO_2, CO, ethanol, and H_2 were monitored as the temperature was raised, continuing until a increase in CO was noted. Figure 4.2 charts the data for the non catalyzed run. Comparison with Figure 21 shows that CO production starts about 50 °C higher in the lead medium, while the hydrogen production and ethanol decomposition are seen to be very similar to the non catalyzed reaction in LBE.
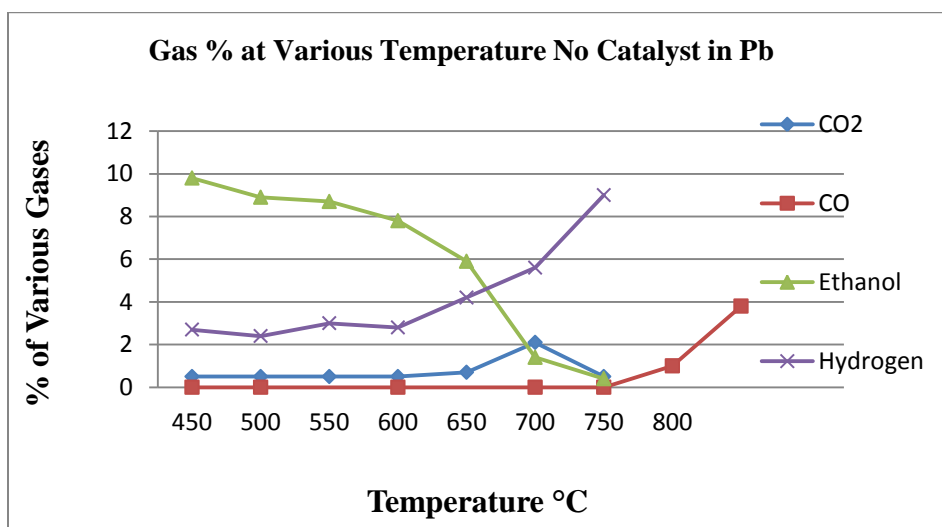
Figure 4.2 Gas % at various temperatures no catalyst in Pb

Again, production of H_2, CO, CO_2, methane, and ethanol decomposition was monitored for each of the catalysts and compared to the non catalyzed reaction. The results of this data are presented in Figures 3.3-3.6. Upon reviewing these results it became immediately apparent the catalysts were having little or no effect in the lead medium.

The initial impression was that some type of coking might be affecting the catalyst performance. However later analysis of the carbon particles collected from the process tube would ultimately offer another explanation which will be discussed in the following chapter.
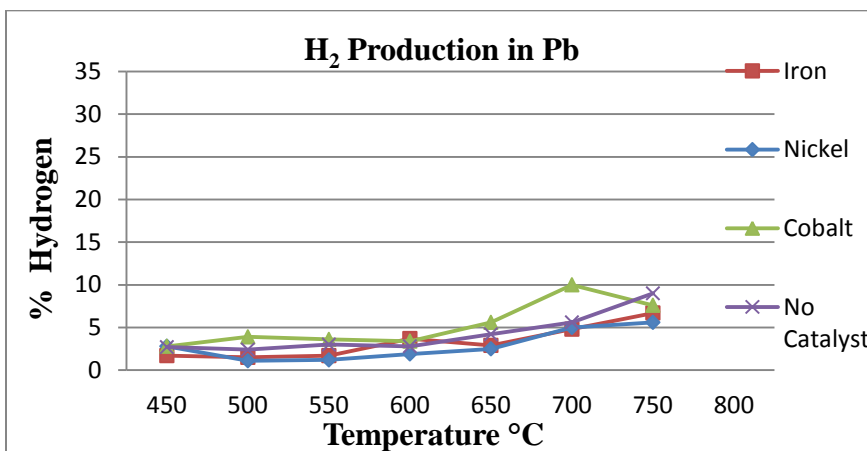
Figure 4.3 H_2 Production in Pb
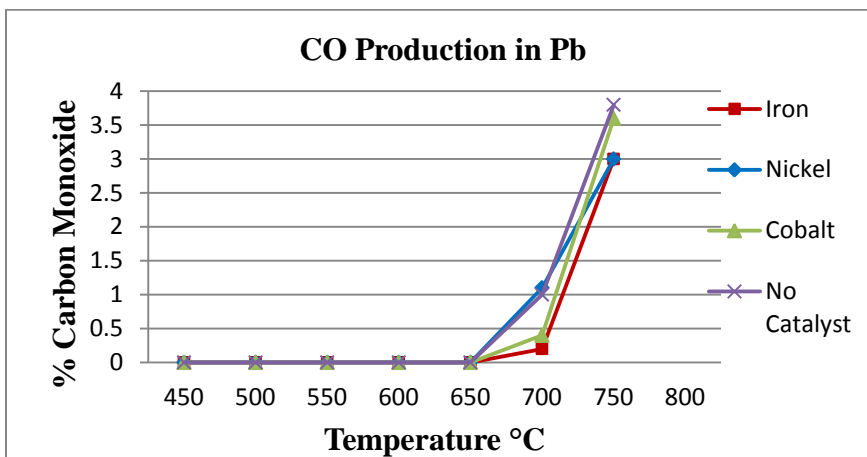
Figure 4.4 CO Production in Pb
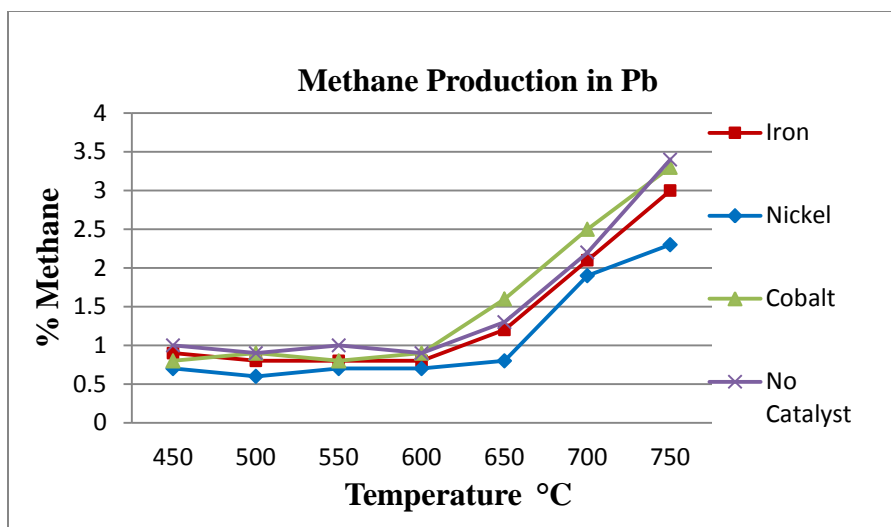
Figure 4.5 Methane Production in Pb
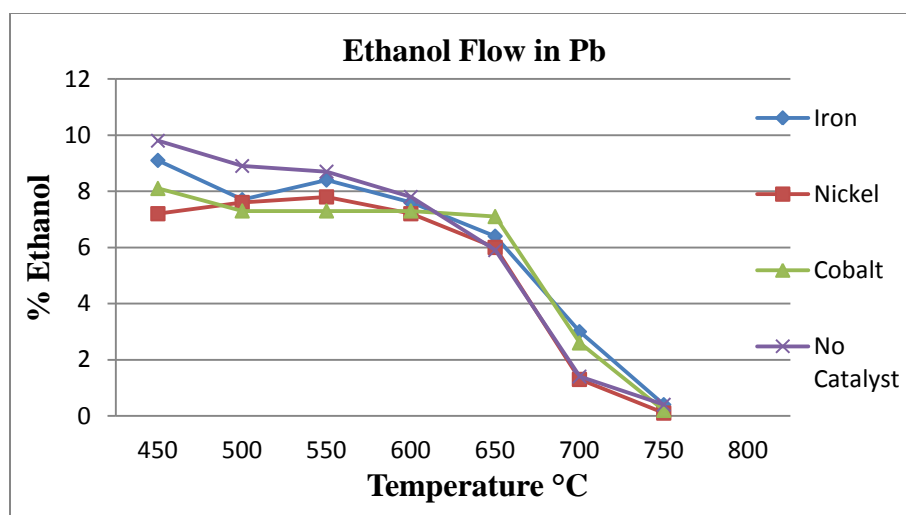
Figure 4.6 Ethanol Flow in Pb

4.4 Discussion of Lead (Pb) Support Testing

When the non-catalyzed testing with lead as the support mechanism produced similar results to the LBE testing; it was anticipated that the catalyzed reactions would also yield results similar to the catalyzed LBE tests. The first catalyzed test run in lead was performed with cobalt due to some favorable results obtained from analysis of the carbon formations produced in the cobalt catalyzed LBE run. Thus, it was somewhat of a surprise that there was no apparent effect on the system when the cobalt catalyst was

introduced into the molten lead. Additionally there was very little carbon forming on the inside of the process tube. It was decided that samples would be collected for future analysis and that testing would proceed with the next catalyst.

Iron was tested next and again spectra indicated that there was little effect when the catalyst was added. At this point it was becoming obvious that the catalyst delivery method did not work the same in lead as it had in LBE. Samples were again collected and the final test using nickel catalyst was performed. As with the previous two cases the addition of the nickel had no discernable effect on the process. It was not until TEM analysis was performed that a viable explanation for this behavior would present itself.

4.5 Additional Testing Results

After the initial data were collected, various parameters were altered or modified in several of the runs. In two of the LBE cases the temperature was taken past the point where CO production was noted. The system was then returned to lower temperature and the production values compared. The reactions continued at basically the same rate or slightly higher rate. In another case, run #6, several failures of the analysis system occurred leaving the data suspect for comparison. However this did afford the opportunity to try a different delivery method for alcohol.

One problem noted with the bubbler set up was that a maximum of about 9% alcohol was seen in the initial spectra. In this case of nickel catalyst in LBE support; complete decomposition of the alcohol was noted before the onset of CO production. Thus it followed that if more alcohol was available for decomposition, more hydrogen could be produced.

In Figure 3.9 (Section 3.5) a small cap on the process gas inlet connection was noted (#3). This cap was used as a place to insert a specially purchased two foot long

hypodermic needle.   The syringe connected to this needle is then controlled with a metering pump, much as a dose of medicine is given to a medical patient hooked up to an IV drip. The cap was a standard compression fitting with a rubber gasket which sealed around the needle after penetration. The tip of the needle is fed down the quartz tube used to deliver feed gas to the system, stopping slightly above the level of the liquid metal support. At this level in the tube the temperature is well above the boiling point of the alcohol, thus it flashes to a vapor.

A rise in the percentage of alcohol delivered to the system is immediately noted with a corresponding reduction in the argon levels.   The manufacturer provides conversion tables based on the syringe size that determine the necessary delivery rate settings and allow them to be changed in mid process. This capability allowed for a gradual increase until the system could no longer decompose the available alcohol.

This particular run was performed using LBE support and iron as the catalyst. The system temperature was adjusted so that the onset of CO production was noted, approximately 0.3%. The alcohol percentage in the spectra was around 1% at this point and it is assumed much of this reading was generated from alcohol present on the walls of the analysis chamber. Hydrogen production in the system was holding around 15% and had not increased when the CO was noted.

The syringe pump (Figure 4.8) was set to deliver the equivalent of what was being picked up in the bubbler. The system was allowed to run four hours under these conditions. Figure 4.7 clearly shows hydrogen production has almost doubled (29.4%) while the alcohol decomposition had actually increased.   On the negative side, an

increase of 1% was also noted in the CO production, indicating finer temperature control will be necessary at increased alcohol feed rates.
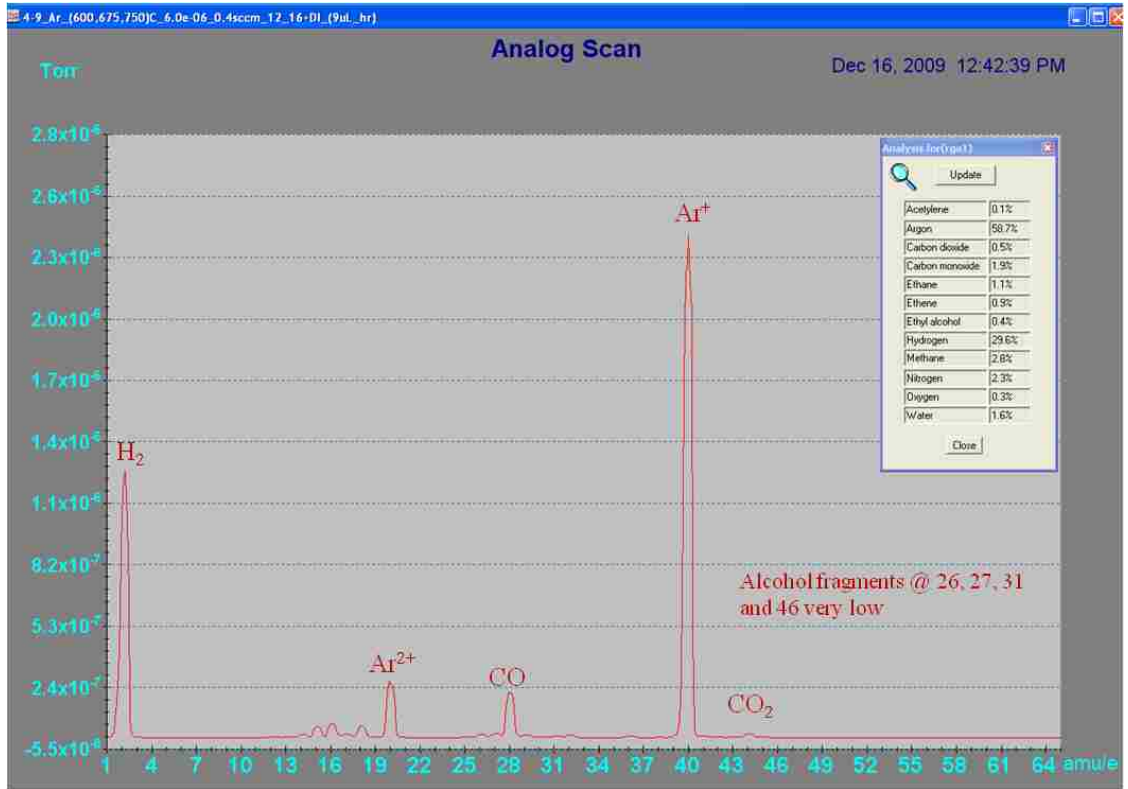

Figure 4.7 Direct injection spectra

Figure 4.8 Direct injection system

CHAPTER 5 CARBON FORMATION RESULTS

Before presenting the results of the carbon formations produced during this testing; it is important to again mention this was an unfunded study on a limited budget. This is noted because analytical testing is very expensive. The preferred method of analysis is TEM (transmission electron microscopy). Although the HRC has a reduced rate for university affiliated research requiring TEM time, the cost for a recent two hour, two sample testing session plus sample preparation and supplies was $350. One hour is only enough time to identify and examine a few of the most prominent concentrations of sample material on the grid. Complete examination of the grid may take many hours of additional analysis. Analysis time can add up especially fast when there are favorable or unanticipated results requiring more in depth analysis. For those not familiar with TEM the following excerpt from the HRC website offers a brief description of the capabilities:

Materials properties and performance of new materials are determined by the presence and interaction of micro structural and nanostructural features such as interfaces and dislocations. Electron microscopy is the primary method to determine structure and chemistry of structural features such as interfaces or dislocations. The Transmission Electron Microscopy Laboratory provides researchers at UNLV with the ability to characterize ceramics, metals, and biological materials at resolutions down to atomic scale (point-to-point resolution = 2 Ångström = 0.2 nm). The Technai F-30 S-TWIN STEM/TEM microscope is operating at 300 kV using a field emission gun in Schottky mode as electron source. This technology provides highest possible resolution of the electron transfer function and of structural features of the material to characterize. Magnifications of typically 1,000,000 times or higher can be achieved. The system allows qualitative chemical analysis with special resolutions of 10 nm using energy disperse X-ray spectroscopy (EDS), parallel energy loss spectroscopy (PEELS), and energy-filtered electron microscopy

(EFTEM). The Technai F-30 is serving as a versatile tool to satisfy the needs of high resolution microscopy in materials science on non-radioactive and radioactive materials [19].

Analysis of a typical sample from our process takes from 1-2 hours for a cursory examination. The small amount of data that will be presented in this section represents between 20-30 hours of analysis time.

Figure 5.1 shows the top of the liquid metal column (LBE) and the 4mm tubes for gas delivery and thermocouple. Additionally, the first signs of carbon production can be seen. The picture was taken a few seconds after the gas was allowed to pass through the alcohol bubbler.
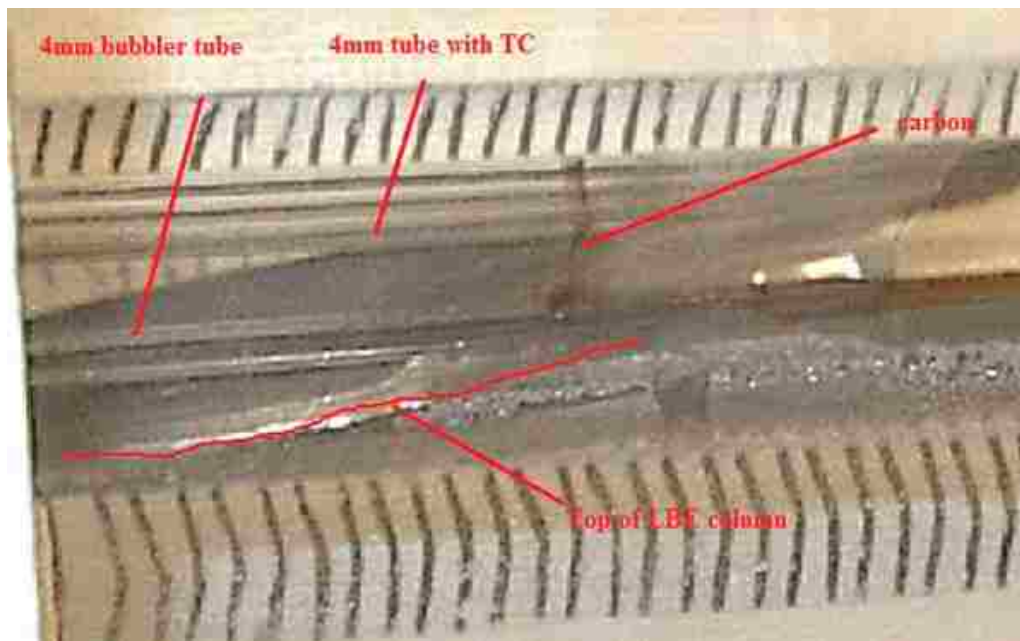

Figure 5.1 Top of liquid metal column (LBE)

5.1 Carbon Background

In general the higher temperature non catalyzed reaction produces an amorphous carbon product in addition to CO gas. Amorphous carbon is the name used for carbon that does not have any crystalline structure. As with all glass like materials, some short-

range order can be observed, but there is no long-range pattern of atomic positions.

Amorphous carbon is formed when a material containing carbon is burned without enough oxygen for it to burn completely. This black soot is known as lampblack or carbon black and is used in the production of inks, paints and rubber products. Additionally, it can also be pressed into shapes and is used to form the cores of most dry cell batteries. Although pure amorphous carbon can be produced; most amorphous carbon actually contains microscopic crystals of graphite or diamond like carbon allotropes [20].

One of the stated goals of this research was to produce a reaction that would have particulate form of carbon as a byproduct. The hope was this product would be a graphite allotrope or possibly a diamond-like allotrope. Either form could have many potential commercial uses.

5.2 Sampling Procedures

The steps used to sample this carbon build up are highlighted in Figure 5.2.

- A rod from a gun cleaning kit was utilized to reach down the tube.
- A piece of sterile lab tissue wetted with ethanol was used as a swab Figure 5.2 (a).
- The sample tissue was then placed in a small vial containing ethanol.
- The vial is then placed in an ultra sonic bath.

Figure 5.2(b) shows the sample after the ultra sonic bath and removal of the tissue. In Figure 5.2(c) the carbon particles have settled on the bottom of the vial. Most of the remaining alcohol is allowed to evaporate leaving a very concentrated sample for analysis.

(a)   (b)   (c)
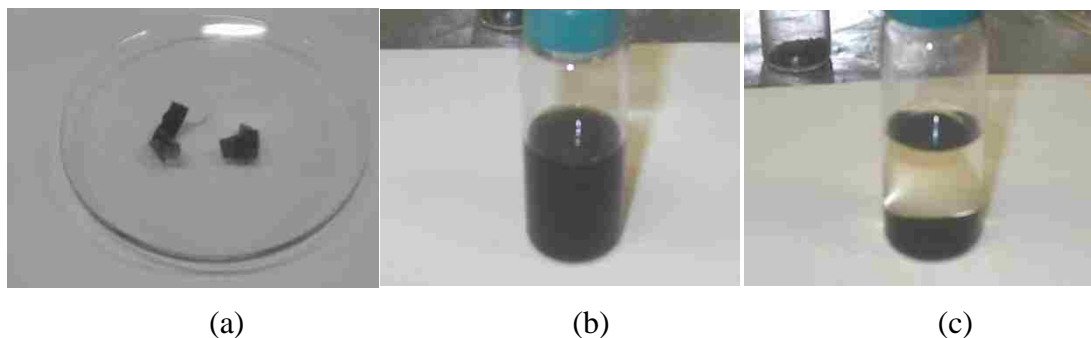
Figure 5.2 Sampling steps

For TEM analysis the sample is shaken and then a dropper is used to place a few drops on the sample holding grid. Figure 5.3(a) shows a general representation of this grid, the actual diameter is about the size of a #2 pencil eraser. This grid is made of copper, thus it is relatively easy to identify during the EDX analysis. Figure 5.3(b) shows another type of grid known as holy carbon, as the name suggests it is made of carbon.

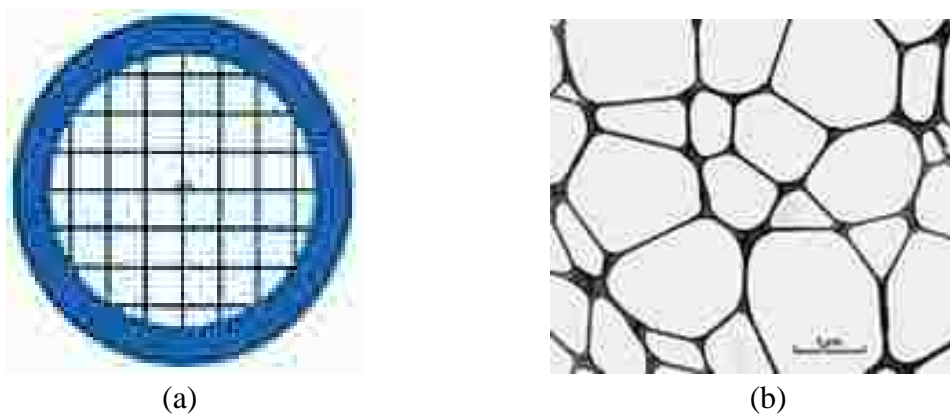(a)   (b)

Figure 5.3 Sample holding grid

5.3 LBE with Ni catalyst

The carbon formations produced by the nickel catalyst were in the form of a fine powder that collected on the inside of the process tube above the liquid metal column. Note that Figure 5.4 shows there is no carbon build up at the interface between the LBE and the quartz process tube.
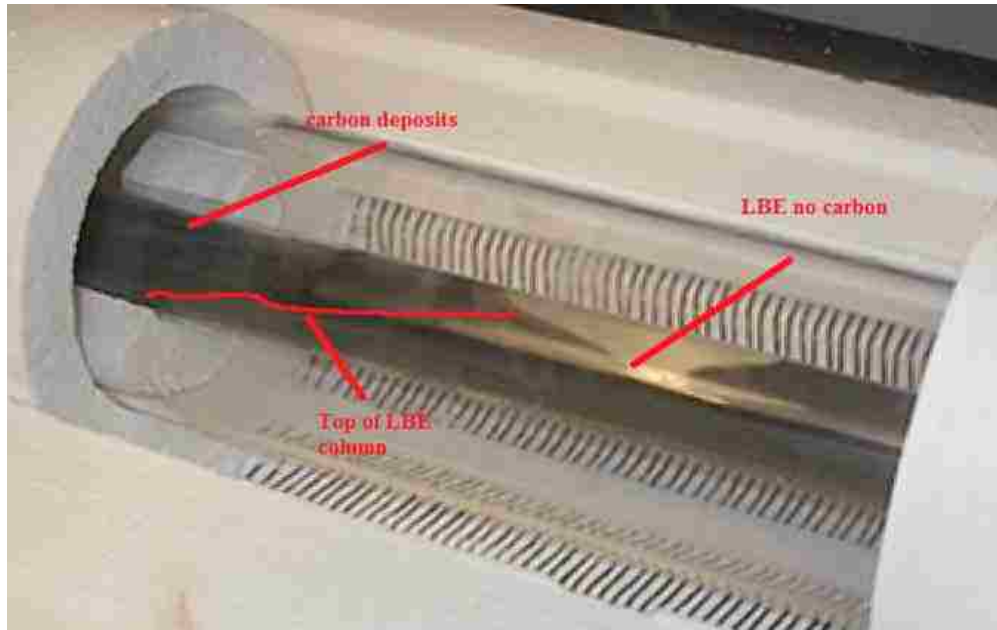
Figure 5.4 Carbon build only above column (Ni catalyst)

TEM analysis shows what is believed to be amorphous carbon with possible crystal type structures [Figure 5.5(a)] and a graphite sheet [Figures 5.5(c), (d)]. The particle seen in figure 5.5(b) was a rather lucky find that turned out to be nickel. Note the approximate size of ~ 10 nm. The scale on the amorphous carbon image (a) is 100 nm. The scales for the graphite images are 20 nm for (c) and 50 nm for (d).

(a)   (b)

<center>(c)   (d)</center>
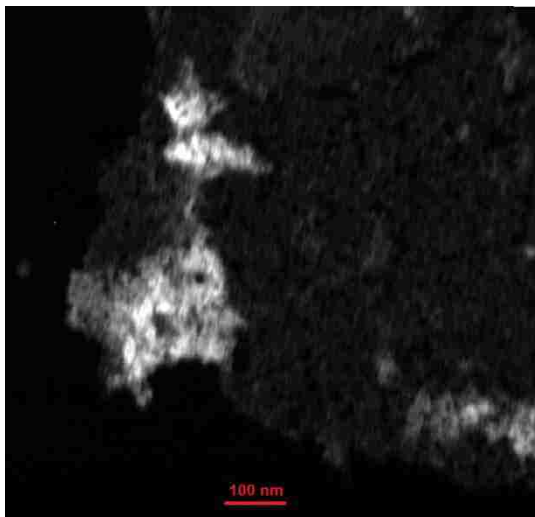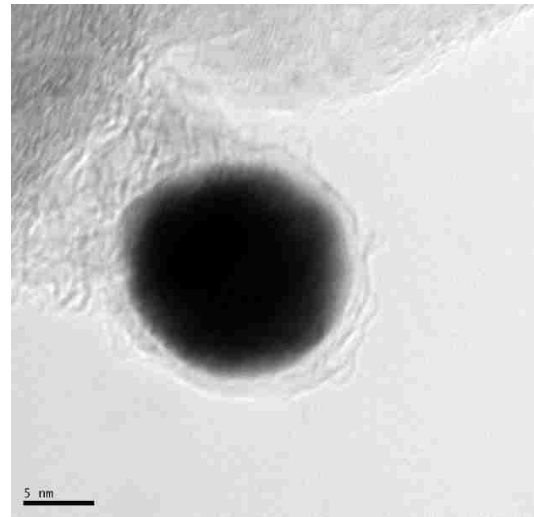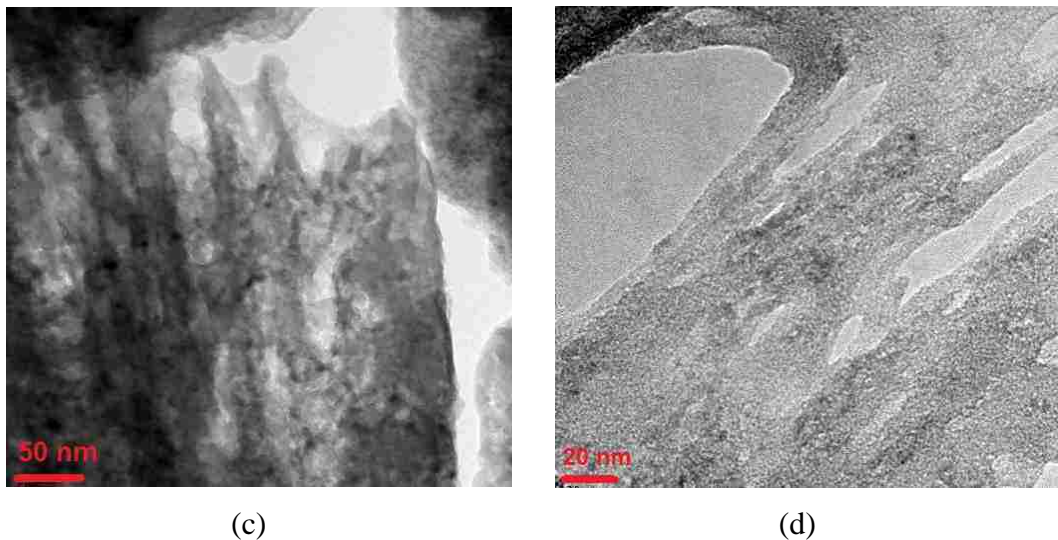
<center>Figure 5.5 TEM imaging LBE with nickel catalyst</center>

Figure 5.6 is the EDX analysis of the particle in Figure 5.4(b).   Energy-dispersive X-ray spectroscopy (EDX) is an analytical technique used for the elemental analysis or chemical characterization of a sample. This technique detects x-rays emitted from the sample during bombardment by an electron beam to characterize the elemental composition.
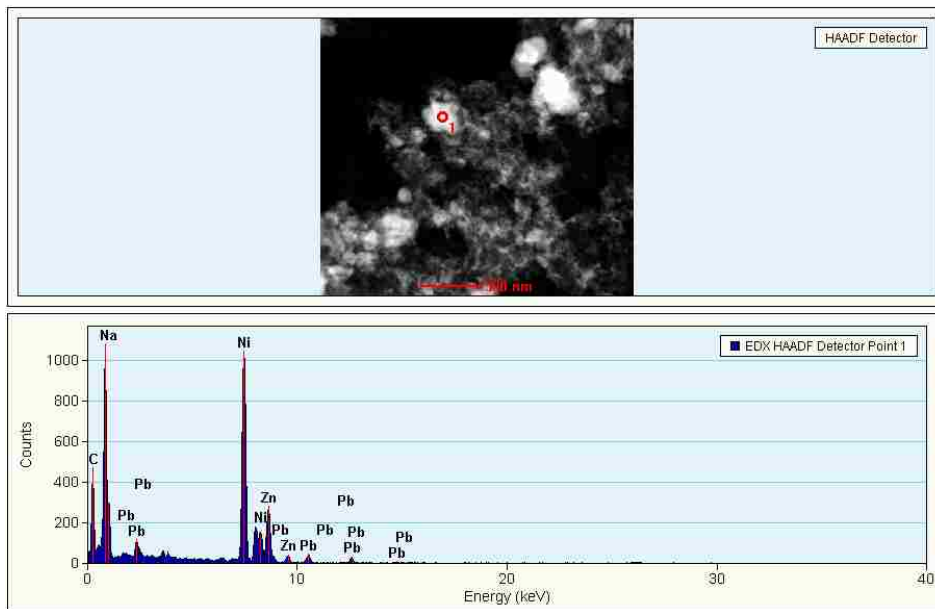
<center>Figure 5.6 EDX spectra LBE with nickel (Ni) catalyst</center>

<center>52</center>

EDX works on the fundamental principle that each element has a unique electronic structure allowing X-rays that are characteristic of an element's atomic structure to be uniquely identified. Two peaks that are identified as nickel are seen at around 7.5 and 8 keV which are consistent with the expected K_α and K_β energies (keV) shown in Table 4. Values of different kinds of transition energies like K_α, K_β, L_α, L_β, and so on for different elements can be found in the NIST X-Ray Transition Energies Database [21].

Table 4 Characteristic X-Ray Energies

(X-ray Energies in keV)								
Z	Element	Ka1	Ka2	Kb1	La1	La2	Lb1	Lb2	Lg1
28	Ni	7.47815	7.46089	8.26466	0.8515	0.8515	0.8688	-	-

5.4 LBE with Fe Catalyst

The iron catalyst testing showed some distinct differences in the carbon product produced as compared with the Ni catalyst. Figure 5.7 shows one of the more dramatic of these differences; a carbon formation at the interface between the LBE and process tube.
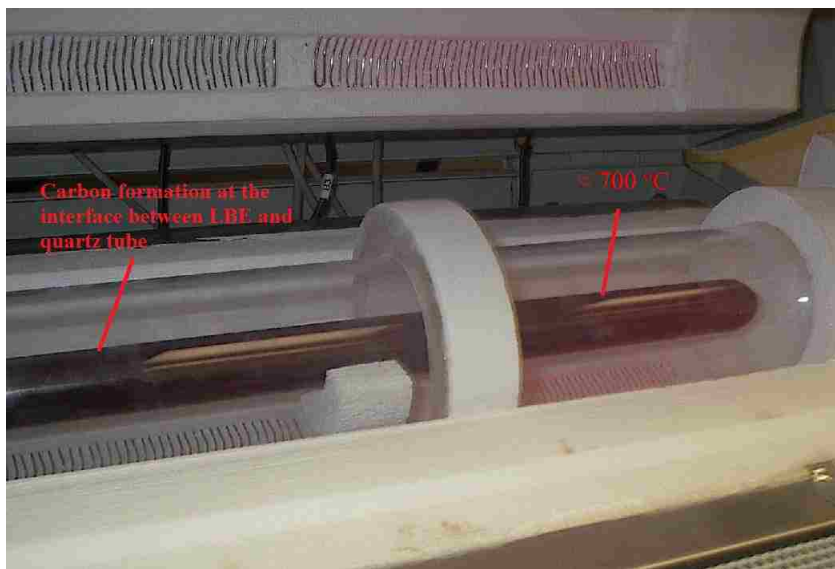
Figure 5.7 Carbon between LBE and quartz tube (Fe catalyst)

The Fe catalyst also produced a "crunchy" carbon deposit with a much larger particle size that collected on the inside of the process tube above the LBE column. The "crunchy" product can be seen in Figure 5.8(a). Figure 5.8(b) shows a piece of the process tube that was in contact with the LBE column. The carbon deposited on the quartz was extremely resistant, when we tried to scrape a sample off, the quartz actually chipped.

(a)   (b)

Figure 5.8 Carbon products LBE with Fe catalyst

Figure 5.9(a) shows a piece of the quartz at 20x magnification with back lighting. Figure 5.9(b) shows a different location, this view has 20x magnification and top lighting. These two locations were specifically chosen to provide contrast; in many areas the carbon coverage was almost complete.
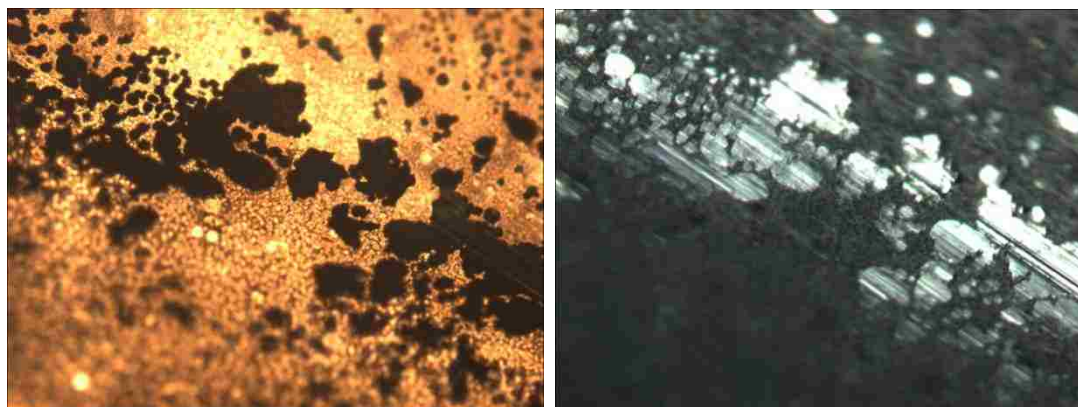
(a)   (b)

Figure 5.9 Carbon products LBE with Fe catalyst

54

The apparent even radial distribution of the carbon build up is of great interest. The initial analysis indicates some type of transfer phenomenon associated with the Fe catalyst as well as relatively even distribution of the catalyst in the LBE.

Figure 5.10(a) shows catalyst wire that did not dissolve into solution indicating the LBE was probably saturated. The small pieces of wire were left in the process tube after pouring off the LBE. Figure 5.10(b) is a 20x magnification of the "crunchy" carbon deposit collected from above the LBE column.

(a)   (b)
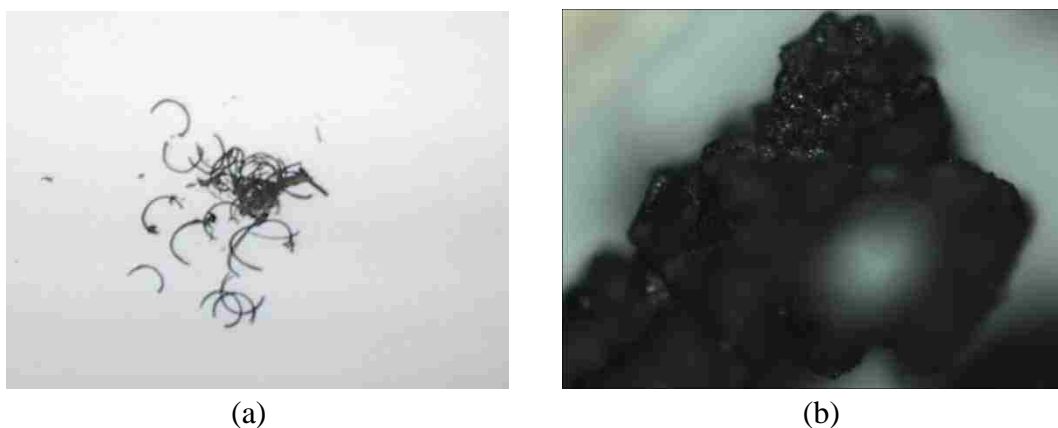
Figure 5.10 Carbon products LBE with Fe catalyst

Figure 5.11(a) is a top lighted 10x magnification of the "crunchy" carbon. Note the small piece of LBE on the right hand side of the image. Figure 5.11(b) is a TEM image of the samples; the scale on this image is 200 nm.

(a)   (b)
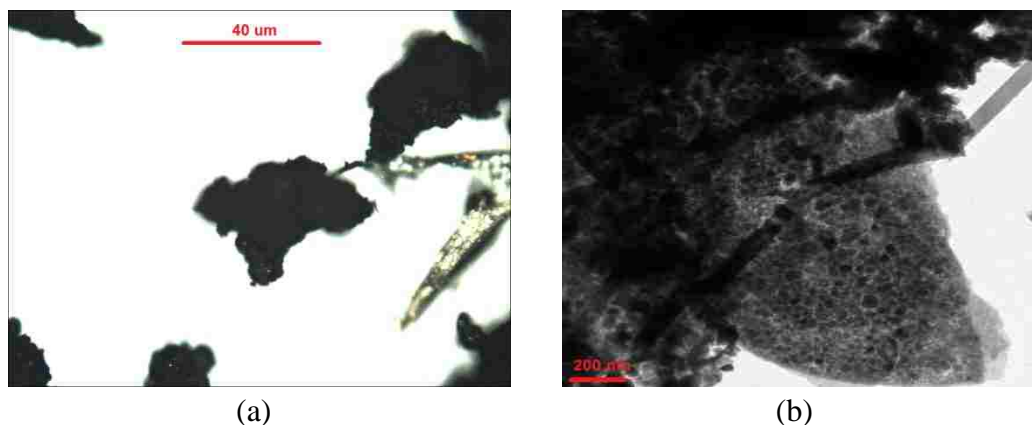
Figure 5.11 Carbon products LBE with Fe catalyst
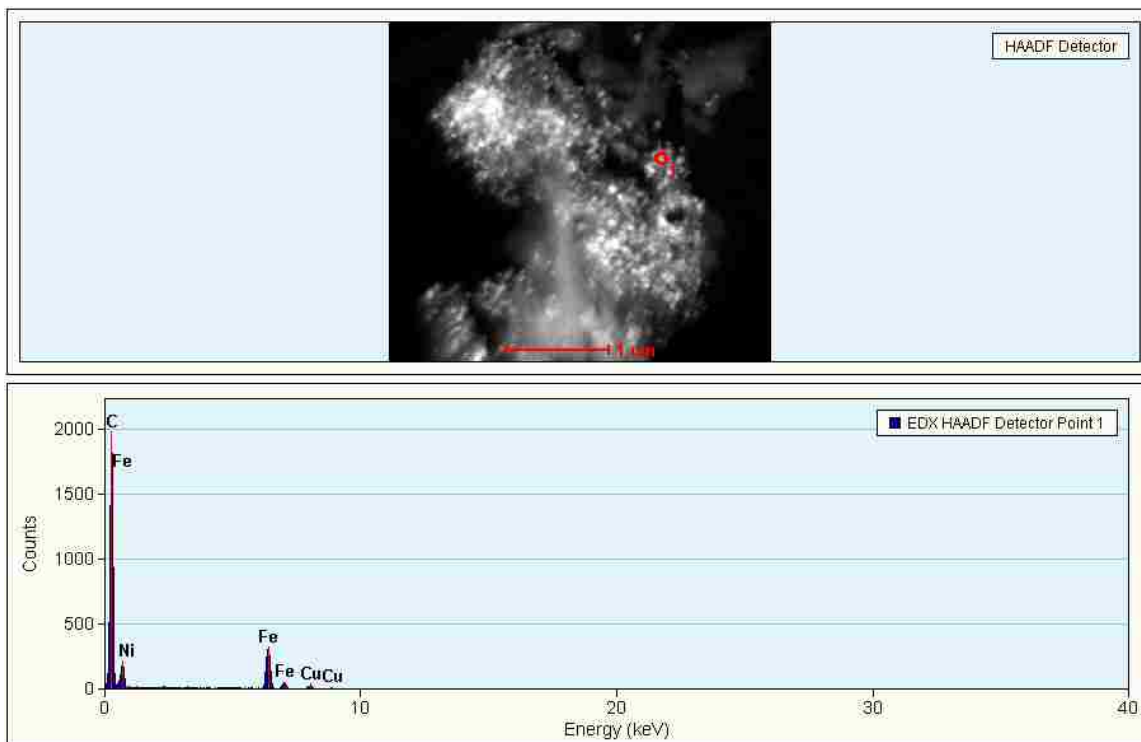
Figure 5.12 EDX spectra LBE with iron (Fe) catalyst

The EDX spectrum shown in Figure 5.12 is from a random sample of the "crunchy" material collected. The spectrum indicates the presence of carbon and iron as expected. This should not be taken as the normal case, finding the iron particle took some searching. The initial analysis has indicated that the Fe catalyst meets the basic goal of sequestering carbon in a particulate form. However the initial data also indicate that a more comprehensive analysis of these carbon forms is necessary to determine if there is any commercial value to this form of carbon byproduct.

5.5 LBE with Co Catalyst

From the standpoint of carbon forms produced; the cobalt catalyst had the most intriguing results. From the beginning of this research it was theorized that the design of the reactor system might produce conditions suitable for the formation of carbon nanotubes. As the testing of the hydrogen production was proceeding very little carbon

buildup was visible on the process tube above the LBE column. There also was no noticeable carbon formation at the interface between the LBE and quartz tube.

The system was allowed to run for several weeks at 675 °C (mean) and over this period it became apparent that there was actually a very fine grey particulate collecting on the process tube above the LBE column. The processed sample was a slightly cloudy liquid. When allowed to settle a very thin layer could be seen at the bottom of the liquid.

The initial reaction was skepticism that any useful carbon formation would be found in this sample. Thus it was a very pleasant surprise when the TEM analysis was performed. Figure 5.13 shows what appear to be carbon nanotubes with multiple catalyst particles. Figure 5.13(a) shows the natural tendency of nanotubes to bundle due to van der Waals attractions, the scale in this image is 50 nm. Figure 5.13(b) shows the tubes interlaced among what is thought to be amorphous carbon.

(a)   (b)
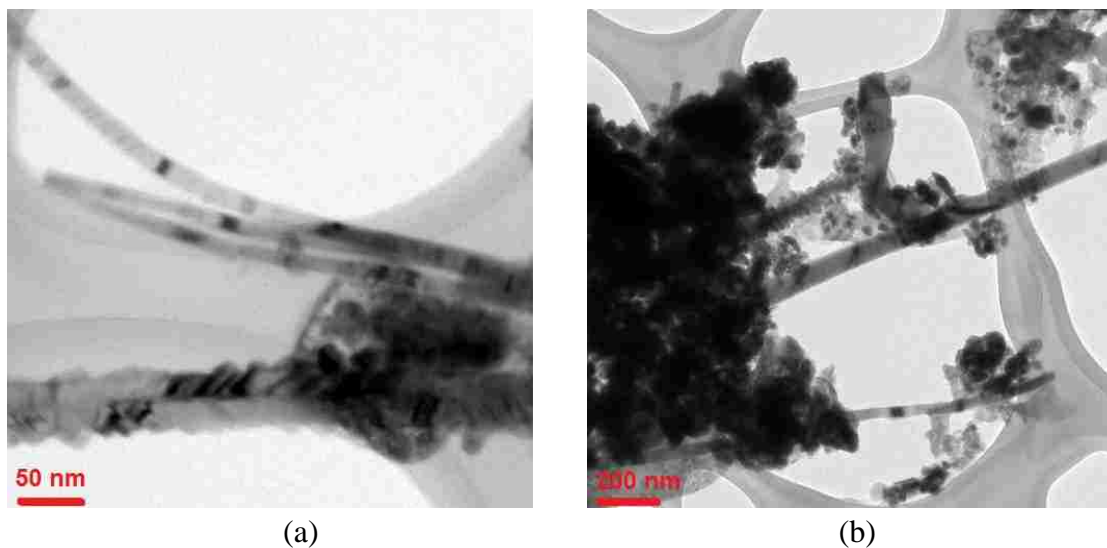
Figure 5.13 Carbon products LBE with Co catalyst

Figure 5.14 shows additional TEM images of individual nanotubes. These lone tubes seem to indicate a good portion of produced tubes may remain suspended in the process gas. This phenomenon also indicates the problems associated with collecting

particles of such small dimensions. This subject will be discussed further in the next

section. It should also be noted this analysis sample was placed on the holey carbon grid

for testing. Also of interest is the varying size of the catalyst particles.

(a)   (b)

Figure 5.14 Carbon products LBE with Co catalyst

Finally, Figure 48 shows an attempt at EDX analysis on one of the tubes. Figure

5.15 shows the analysis of a spot where it was believed a catalyst particle would be.
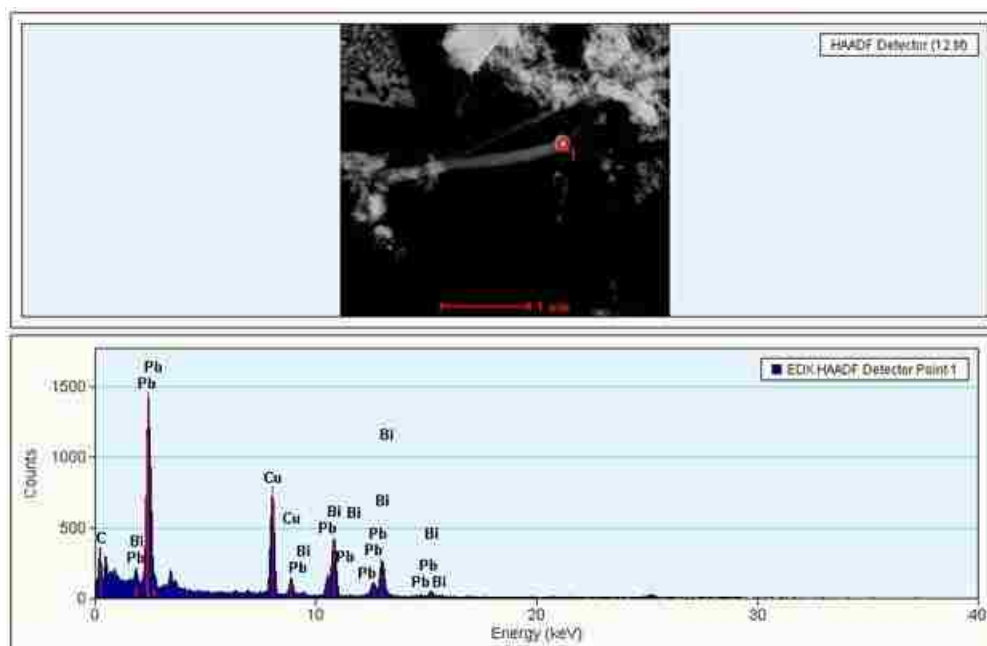
Figure 5.15 EDX spectra LBE with Co catalyst

This spot actually turned out to be a particle of LBE behind the tube. Here it is important to note the difficulty in determining the orientation of the spot being analyzed. In a thorough analysis the same spot would be analyzed from several different angles. The TEM is capable of running a grid type search, however this 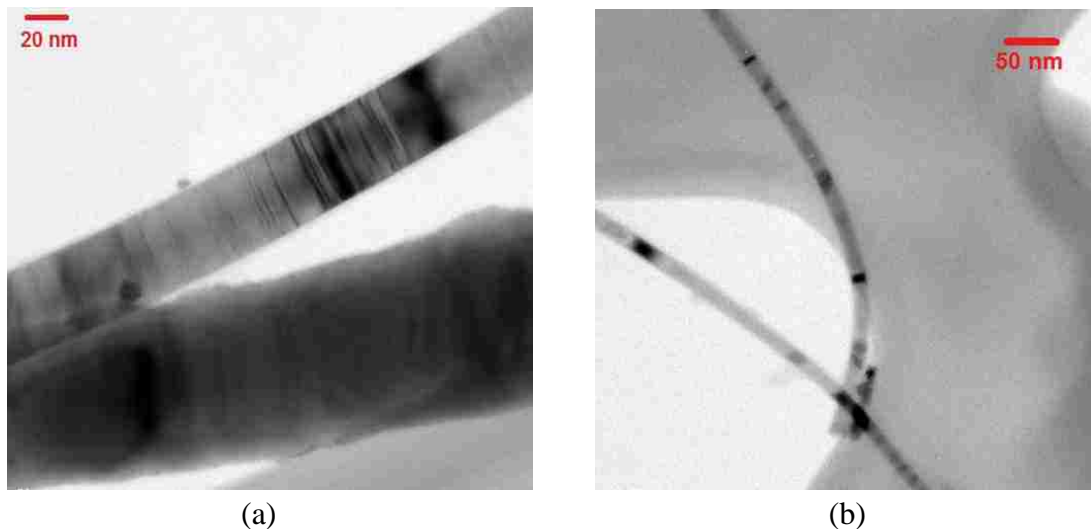is time consuming and thus is also expensive. Testing of the properties of these tubes will obviously be a complicated and expensive process.

5.6 Lead (Pb) Carbon Formation Results

When doing investigative research of this type it is important to remember; a negative result still provides data. From this point of view the testing in the lead medium is what NASA used to call; "a successful failure". The catalyzed reaction did not produce the desired results for hydrogen production; however interesting results were obtained on the behavior of the catalyst particles and reaction products.

In both the nickel and cobalt catalyzed tests, the process tubes had only a slight visible build up. Following the same procedures outlined earlier, sample swabs were taken from the inside of the process tube for TEM analysis. Figure 5.16 shows two images of the nickel catalyzed sample.

(a)   (b)
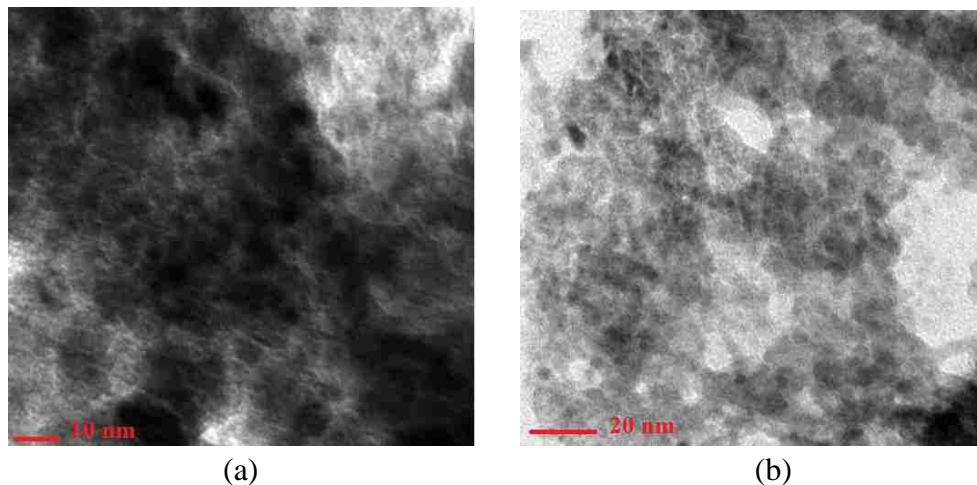
Figure 5.16 Carbon products Pb with Ni catalyst
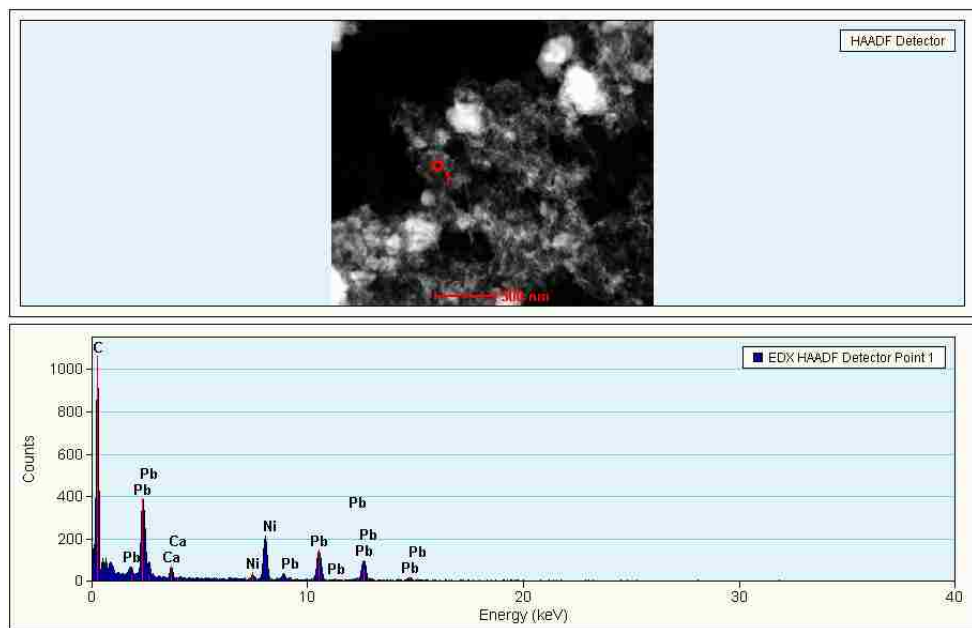
Figure 5-17 EDX spectra Pb with Ni catalyst

The EDX spectrum in Figure 50 is the analysis of the sample area shown of Figure 49(b). The spectrum indicates the presence of lead, carbon, and nickel. While the catalytic particles appear to be fairly evenly distributed, the analysis seems to indicate the particles are coated with a thin layer of lead. Earlier in this paper it was mentioned that many catalytic reactions experience a drop in performance over time due to coking.

Coking is a process that covers the catalyst in polymeric by-products, this process effectively isolates the catalytic particle from the reaction medium. The catalytic particles seem to have experienced a similar effect in the lead medium, however it is believed that a different root cause is responsible, the reasoning of which will be discussed in Chapter 6.

Figure 5.18 shows TEM images of the cobalt catalyzed sample which appears very similar to the nickel catalyzed images. Figure 5.19 shows that the EDX analysis also produced spectra similar to the Ni results; again this seems to indicate the catalyst is basically trapped in mixture of carbon and the lead medium.

60
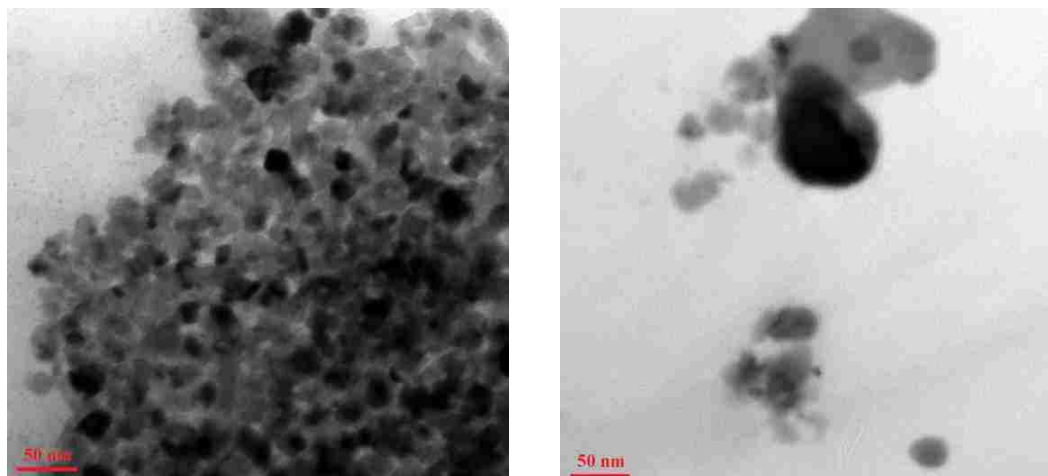
| (a) | (b) |

Figure 5.18 Carbon products Pb with Co catalyst
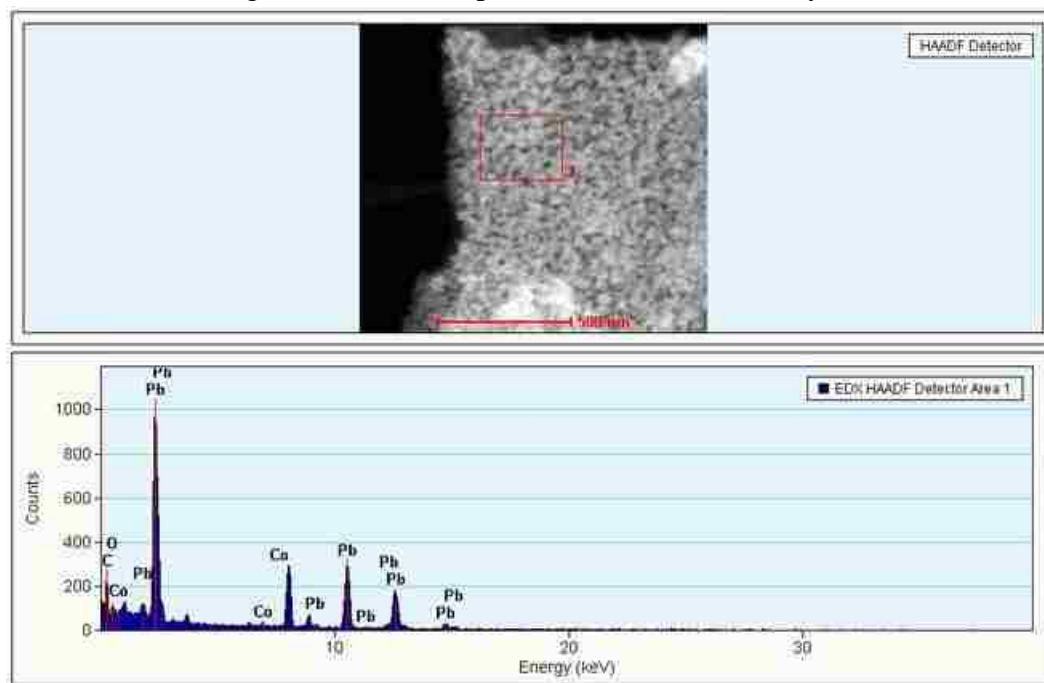
Figure 5.19 EDX spectra Pb with Co catalyst

The testing of the Fe catalyst in the lead medium also showed very poor performance from the standpoint of hydrogen production. In contrast the process tube was visually very similar to what was seen in the LBE testing. The interface between the lead and quartz tube also experienced the formation of a buildup that appear to be carbon.

Additionally there appeared to be a buildup of a particulate form of carbon above the lead column. Figures 5.20(a), (b) show the TEM images of this sample which again appears very similar to the NI and Co catalyzed samples.

(a)   (b)   (c)
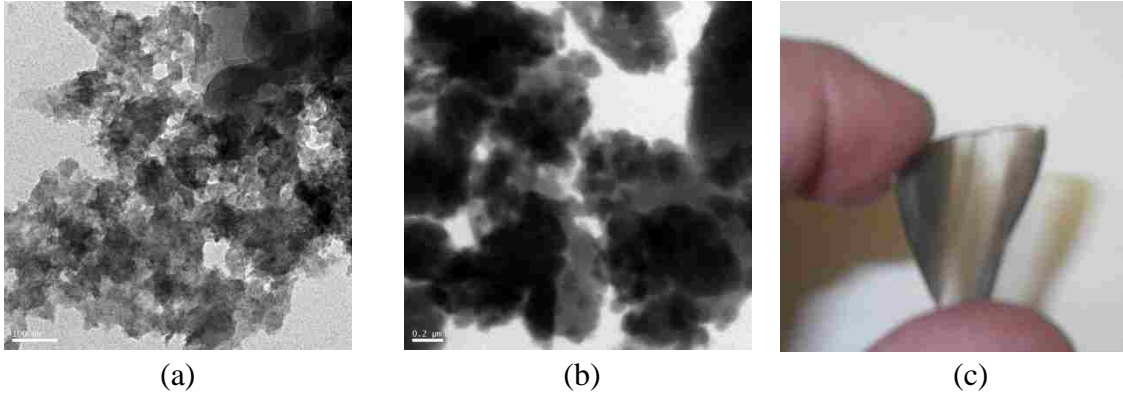
Figure 5.20 Carbon products Pb with FE catalyst

Figure 5.20(c) is a picture of the piece of the process tube from the same area as where the sample swab was taken. Figure 54 is a 20x magnification of this piece, (a) is a backlit, and (b) is top lighted.   These images show the buildup pattern to be quite different from what was seen in the LBE test (see Figures 5.21a, b).

(a)   (b)
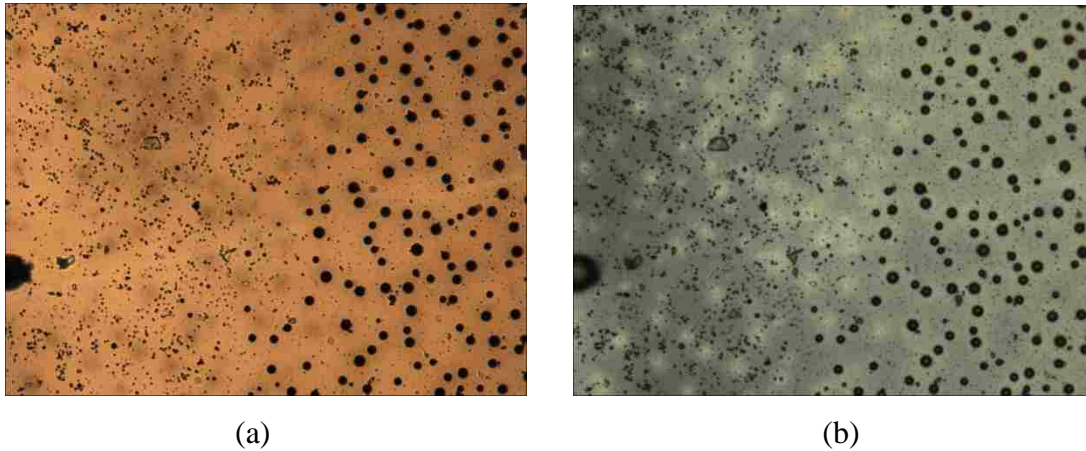
Figure 5.21 Carbon products Pb with FE catalyst

Figure 5.22 shows the back and front lighted views of a piece of the process tube in contact with the lead column. This 10x magnification shows a very different form of buildup is produced. Visually from the outside; the tube appeared to have the same black

carbon build up seen in the LBE testing. In contrast the microscopic analysis of the interior of the tube shows what appears to be a metallic layer.

(a)   (b)

Figure 5.22 Carbon products Pb with FE catalyst

Figure 5.23 is a 20x magnification of the same sample showing what is believed to be mixture of lead, Fe particles, and an underlying carbon layer. Further analysis outside of scope of this work is planned using XPS and will be further addressed in the conclusions. The bright blue color is believed to be an oxide layer formed when the lead was poured out of the process tube and remaining layer was exposed to air.

Figure 5.23 Carbon products Pb with FE catalyst

CHAPTER 6 CONCLUSIONS AND FUTURE WORK

When reviewing the data generated by this study it becomes clear this project was an overall success in the fact that all of the major goals proposed at the start of this research were met.

The first of these goals was the design and testing of a reactor capable of the high temperature decomposition of ethanol. Further the system design required the capability of lower temperature non-isothermal testing of catalyzed reactions. Like any testing apparatus this system required some adjustments as testing proceeded, however the design proved more than satisfactory for stated goals. Additionally, the system was found to be exceedingly easy to adapt for additional testing not initially anticipated, such as the direct injection experiments.

The second goal was to initiate a catalyzed ethanol decomposition reaction that produced hydrogen without CO gas as a byproduct, but rather sequestering the carbon in a particulate form. This portion of the testing showed a 50% success rate and a 50% successful failure rate. From a hydrogen production point of view; the testing using LBE as the liquid metal support was a complete success. All three of the tested catalysts initiated a lower temperature reaction producing hydrogen, water, and solid carbon as byproducts without the presence of CO gas. However, from a hydrogen production point of view; the testing using lead as the liquid metal support was a failure.

This was offset when viewing the results from a catalyst delivery point of view. The lack of catalytic reaction in the lead medium and the subsequent analysis indicating the catalytic particles had become coated in lead was quite significant. The additional discovery of the metallic layer observed on the inside of the process tube during the lead

64

testing indicates something unique is occurring in the catalyzed eutectic. One of the problems with catalysts is they want to react, and unfortunately they do not always react in the anticipated way. A great deal of time and money are devoted to the study and manipulation of catalytic reactions. This type of testing is empirical in nature, and as seen in these results quite situation dependant.

After examination of the data it is believed there is a relatively simple explanation for the differences seen in the behavior of the catalysts in the LBE and lead mediums. First it is important to remember that LBE is a eutectic alloy composed of (44.5%) lead and (55.5%) bismuth.

The change in catalytic behavior between the liquid lead and the liquid LBE case can be understood by examining the stability of each phase that is present. The phase of lowest energy is the one that is seen. In this system, we need to look at solid lead, liquid lead and LBE, and lead on the surface of the catalytic metals.

One result of the difference in stability as a function of temperature is melting behavior − as the temperature increases, the entropy of the liquid is favored over the lower entropy of the solid. The low melting point of LBE indicates that with respect to solid lead (and bismuth), LBE liquid is remarkably stable, as shown by its melting point of 123 °C. Lead adsorbed onto the catalyst metals is expected to be more stable than a pure lead surface. Thus, catalytic metals in liquid lead are covered by a layer of lead. As a result, all of the catalytic metals act similarly with respect to the pyrolysis of ethanol.

However, the lead in LBE is stabilized by alloying with bismuth (giving it its low melting point), and apparently is more stable than lead on the catalytic metals at reaction temperature, so a clean catalytic metal surface is available for catalytic work. This

phenomenon indicates a more in-depth study of the behavior of catalysts in LBE and other eutectics is order.

Further, future testing for the production of hydrogen should include the examination of different eutectics as the liquid metal support. The catalyst coating problems encountered in the lead medium testing actually helped show the validity of the proposed delivery of catalyst material in LBE, which was the third goal of this research.

The final goal of this research was to examine the carbon byproducts produced by the catalyzed reactions for potential commercial uses. It was deemed possible the reactor design might provide conditions favorable to the formation of carbon nanotubes and other carbon forms from the graphite family. The initial data indicate the cobalt catalyst provided the proper size particles for the formation of nanotube like structures. Also of interest were the graphite sheet structures found in the Ni catalyst testing in LBE.

Due to the favorable results obtained in LBE with a cobalt catalyst, a second round of testing with this combination is currently being performed, unfortunately the results of which will not be known until after the presentation of this work.

One rather unanticipated result was the formation of a carbon layer at the interface of the LBE and quartz during the Fe catalyst testing. This process might have potential as a highly resistant coating able to endure high temperatures and bears further investigation also.

One clear result that can be seen from the data generated is that the catalyzed reactions in LBE occurred at a temperature low enough that CO gas was not produced as a byproduct. Further, the data show the major byproducts of this reaction to be hydrogen, water, and solid carbon forms. The data have also indicated that the choice of catalyst is

of great importance in both the production hydrogen and the formation of specific carbon species. Thus, whichever direction further studies take should funds become available for additional testing; the first step should be a thorough study of the behavior of catalysts in a liquid metal support systems. Particular attention should be given to liquid metal eutectics.

If further studies center around hydrogen production it is suggested that the catalytic studies first examine nickel and nickel compounds, possibly followed by more exotic materials such as platinum and palladium. Testing should include examination of the effects of varying the amount of catalyst present in the system; as well as the effects of varying the amount alcohol available for decomposition. The direct injection process tested worked well in initial testing for raising the available percentage of alcohol. The second generation reactor used in this testing has proved quite effective for the testing of the catalytic reactions and should continue to be used for this propose.

The initial hydrogen testing data also indicate an increase in both contact time and contact area is desirable. Additionally the third generation reactor design must increase in size for this process to be commercially viable. To address these issues it is believed the design of the third generation reactor should be similar to a commercial distilling column. A system is proposed that will allow the catalyst impregnated liquid metal to be released at the top of the column as either an aerosol or as droplets formed by a diffusion plate. These small droplets of medium would be allowed to fall through a heated carrier gas saturated with ethanol. Converting the medium to small drops increases the surface per given mass and the tall column provides increased contact time.

In theory the proposed gravity column design should also allow the carbon formations to easily separate from liquid metal droplets as the fall. For the formation of nanotubes this separation would be highly desirable. The tubes and attached catalytic particle should be highly buoyant and want to float upward in the saturated carrier gas. It is hoped that this contact time will allow for continued growth of the tubes.

In summary we can see that this research has raised many new questions and avenues of approach for further studies. Having a working system in place makes continued testing of catalysts the most practical direction to pursue. However this is a time consuming process that should be run in parallel with further research of the carbon formations. A relatively modest budget (by research standards) would allow for continued lab scale research. This would include the building of additional test reactors to produce samples and compressive analysis of the samples using TEM and other analytical methods.

While it is our belief this process shows great promise as a commercially viable way to produce hydrogen as a feed stock or fuel; continued research in this direction would require more substantial budget. Although the process should be easily scalable; to be practical use the system design must also be easily integrated into existing thermal dissipation technologies.

REFERENCES

[1] Universal Industrial Gases, Inc. **http://www.uigi.com/hydrogen.html** (accessed June 7, 2010).

[2] Albert Casanovas, Maider Saint-Gerons, Fabien Griffon, Jordi Llorca, "Autothermal generation of hydrogen from ethanol in a microreactor", International Journal of Hydrogen Energy, Vol. 33, pp. 1827 – 1833, (2008).

[3] Kuen-Song Lin, Cheng-Yu Pan, Sujan Chowdhury, Mu-Ting Tu, Wan-Ting Hong and Chuin-Tih Yeh, "Hydrogen Generation Using a CuO/ZnO-ZrO2 Nanocatalyst for Autothermal Reforming of Methanol in a Microchannel Reactor", Molecules, V16, pp. 348-366, (2011).

[4] Wikipedia. http://en.wikipedia.org/wiki/Hydrogen_production (accessed May 9, 2010).

[5] Jordi, L., N. Homs, J. Sales and P. Ramirez de la Piscina, " Efficient Production Of Hydrogen over supported Cobalt Catalysts from Ethanol Reforming," Journal of Catalysis, 209, pp. 306-317 (2002).

[6] Leclerc, S., R.F. Mann and B.A. Peppley, "Evaluation of the catalytic ethanol-steam reforming process as a source of hydrogen-rich gas for fuel cells", Prepared for the CANMET Energy Technology Centre (CETC), (1998).

[7] Galvita, A.A., G.L. Semin, V.D. Belyaev, V.A. Semikolenov, P.Tsiakaras and V.A. Sobyanin, "Synthesis gas production by steam reforming of ethanol", Applied Catalysis A: General 220, pp. 123-127, (2001).

[8] Claudia Esarte, María Peg, María P. Ruiz, Angela Millera, Rafael Bilbao, and María U. Alzueta, "Pyrolysis of Ethanol: Gas and Soot Products Formed", Industrial & Engineering Chemistry Research, 50, pp. 4412-4419, (2011).

[9] Sarahssureshots. http://sarahssureshots.wikispaces.com/Focus+on+Proteins (accessed August 11, 2011).

[10] Dr. Eric Loewen, GE Hitachi Nuclear Energy (GEH) chief consulting engineer for advanced plants technology. Formerly with Idaho National Laboratory (molten lead cooled reactor project). http://local.ans.org/virginia/meetings/2011/loewen.html (accessed June 14, 2011).

[11] Raymond M. Reilly, "Carbon Nanotubes: Potential Benefits and Risks of Nanotechnology in Nuclear Medicine", The Journal of Nuclear Medicine, Vol. 48 no. 7, pp. 1039-1042, (2007).

[12] K.Safarova, A.Dvorak, R. Kubinek, M.Vujtek, A. Rek, "Usage of AFM, SEM and TEM for the research of carbon nanotubes", Modern Research and Educational Topics in Microscopy, V1, pp. 513-519, (2007).

[13] Gary G. Tibbetts, "Carbon fibers produced by pyrolysis of natural gas in stainless steel tubes", Applied Physics Letters, Vol. 42. No.8., pp. 15, (1983).

[14] Ajayan, P. M.; Zhou, O. Z., "Applications of carbon nanotubes", Carbon Nanotubes, Vol. 80, pp. 391-425,(2001).

[15] Aliev, et al., "Giant-Stroke, Super elastic Carbon Nanotube Aero gel Muscles", Science, Vol. 323, no. 5921, pp. 1575-1578, (2009).

[16] Wikipedia. http://en.wikipedia.org/wiki/Carbon_nanotube (accessed May 23, 2009).

[17] H. Glasbrenner, F. Groschel, H. Grimmer, J. Patorski, M. Rohde, "Expansion of solidified lead bismuth eutectic", Journal of Nuclear Materials, 343, pp.341–348 (2005).

[18] Stanford Research Systems, "Operating and Programming Reference", Revision 1.6 (2005).

[19] HRC website. http://nstg.nevada.edu/TEM/TEM.htm (accessed September 3, 2011).

[20] B. A. Movchan and A. V. Demchishin, "Study of the structure and properties of thick vacuum condensates of nickel, titanium, tungsten, aluminum oxide and zirconium dioxide", Phys. Met. Metallogr, 28: 83–90, (1969).

[21] NIST X-Ray Transition Energies Database. http://www.nist.gov/pml/data/xraytrans/index.cfm (accessed September 3, 2011).

Peter Faught

4640 Koval Ln. #40B
Las Vegas, Nv 89109
702-319-1653
faughtnevada@cox.net

Personal

Born June 29, 1963 in Cheyenne Wyoming. Las Vegas Resident since July 1996.

Education

BSME Howard R. Hughes College of Engineering, University of Nevada Las Vegas. Emphasis on manufacturing processes and systems, regulatory compliance, and lean manufacturing.

Bobcat Ltd. Hydraulic systems Certification course. Course work included pump and cylinder rebuild as well as hydraulic power transfer theory.

Associated Building Contractors electrical apprentices program, Denver Co. Course work was designed for commercial electrical licensing.